NJC

Accepted Manuscript

This is an *Accepted Manuscript*, which has been through the Royal Society of Chemistry peer review process and has been accepted for publication.

Accepted Manuscripts are published online shortly after acceptance, before technical editing, formatting and proof reading. Using this free service, authors can make their results available to the community, in citable form, before we publish the edited article. We will replace this *Accepted Manuscript* with the edited and formatted *Advance Article* as soon as it is available.

You can find more information about *Accepted Manuscripts* in the Information for Authors.

Please note that technical editing may introduce minor changes to the text and/or graphics, which may alter content. The journal's standard Terms & Conditions and the Ethical guidelines still apply. In no event shall the Royal Society of Chemistry be held responsible for any errors or omissions in this *Accepted Manuscript* or any consequences arising from the use of any information it contains.

ROYAL SOCIETY OF CHEMISTRY

www.rsc.org/njc

Journal Name

RSCPublishing

ARTICLE

Five Novel Dicyanidoaurate(I)-Based Complexes Exhibiting Significant Biological activities: Synthesis, Characterization and Three Crystal Structures

Cite this: DOI: 10.1039/x0xx00000x

Received 00th.....2014,
Accepted 00th.....2014

DOI: 10.1039/x0xx00000x

www.rsc.org/

Ahmet Karadağ,[a]* Ali Aydın.[b] Süreyya Dede.[a] Şaban Tekin.[b] Yusuf Yanar.[c] Bilge Hilal Çadırcı.[d] Mustafa Serkan Soylu.[e] Ömer Andaç.[f]

Five new cyanido-bridged coordination polymers having closed formulas [Ni(*hydeten*)$Au_2(CN)_4$] (**C1**) [Ni(*hydeten*)$_2Au_2(CN)_4$].H_2O (**C2**), [Cu(*hydeten*)$_2Au_2(CN)_4$].CH_3OH (**C3**), [Zn(*hydeten*)$_2$ $Au_2(CN)_4$].H_2O (**C4**), and [Cd(*hydeten*)$_2Au_2(CN)_4$].H_2O (**C5**). (*hydeten:*N-(2-hydroxyethyl)-ethylenediamine) have been prepared and characterized by elemental, thermal, FT-IR and XRD (**C3**, **C4** and **C5**) measurement techniques. The anticancer, antibacterial and antifungal activities of the complexes are also investigated. The **C3**, **C4** and **C5** units according to XRD analyses are linked to each other via –CN–M(*hydeten*)–NC–Au(1)–CN–M(*hydeten*)–CN– chains (M^{II}= Cu, Zn and Cd) and aurophilic interacted –Au(1)(CN)2–Au(2)(CN)2–Au(1)(CN)2–Au(2)(CN)2– zig-zag shaped chains along the *a* axis. **C1**, **C2** and **C4** show significant antifungal effects against several plant pathogenic fungi, while surprisingly **C3** exhibits considerable antibacterial effect against gram negative *E. coli*. The antiproliferative activity studies on Hela, HT29 and *C6* tumor cell lines indicated anticancer potential of even at low doses.

INTRODUCTION

Coordination polymers exhibiting characteristics such as conductivity,[1,2] magnetic[3-10] and porosity[11-13] have been recently investigated due to their potential of generating such materials. Coordination polymers resulting from the assembly of molecular building blocks are composed of metal ions, capping ligands and bridging ligands. Cyanido-bridged complexes dicyanidometallate and tetracyanidometallate-based constitutes an important member of the coordination polymers class.

Bimetallic supramolecules containing cyanidometallate building blocks have become the focus of attention of researchers because of their interesting structures and diverse features. The dicyanidoaurate(I) building block, $[Au(CN)_2]^-$, found among cyanidometallates has been used in the construction of *2D* and *3D* coordination polymers because of Au·····Au aurophilic interaction playing a key role in controlling the dimensionality and topology. [14-18] Despite the possibility to exhibit properties such as luminescence,[19-22] vapochromism[23,24] and magnetism[25-27] of the cyanidoaurate-based coordination polymers, they also have important industrial[28] and medical applications.[29,30]

Hydeten, (N-(2-hydroxyethyl)-ethylenediamine; alternatively named 2-(2-aminoethylamino)-ethanol, $H_2NCH_2CH_2NHCH_2CH_2OH$) used as capping ligand in this study is acting as a bidentate ligand through its two nitrogen donor sites[31-37] and a tridentate ligand via its all three donor centers.[38] In our earlier study,[39] it was used to obtain the dicyanidoargentate(I)-based two cyanido complexes and the structures have been shown to act as a bidentate ligand of *hydeten*.

The purpose of this study is to investigate the biological (anticancer, antimicrobial and antifungal) activities of the dicyanidoaurate-based new coordination polymers obtained by using Ni^{II}, Cu^{II}, Zn^{II} and Cd^{II} ions and *hydeten*. Previously, we showed that $[Ni(hydeten)_2Ag(CN)_2][Ag(CN)_2].H_2O$, $[Cd_2(hydeten)_2Ag_4(CN)_8].H_2O$, [39] $[Cd_2(edbea)_2][Ag(CN)_2]_2.H_2O$, {*edbea:* 2,2'-(ethylenedioxy) bis(ethylamine)} and $[Ni(N\text{-}bishydeten)Ag_3(CN)_5]$[40], {*N-bishydeten: N,N*-bis(2-hydroxyethyl)-ethylenediamine} complexes possess remarkable biological activities. Similarly, the novel complexes of this study; **C1**, **C2**, **C3**, **C4** and **C5** have shown quite significant biological activities *in vitro*. In particular, it can be stated that these complexes have remarkable anticancer activities on studied cancer cells. According to present literature, this is the first study investigating biological activities of the dicyanidoaurate-based complexes.

RESULTS and DISCUSSION

C1, **C2**, **C3**, **C4** and **C5** Containing *N,N*-bis(2-hydroxyethyl)-ethylenediamine and $[Ag(CN)_2]^-$ were prepared according to methods known as "*brick-mortar*". The polymeric structures of **C3**, **C4** and **C5** containing H_2O excluding **C3** (CH_3OH) in the crystal lattices were determined by X-ray single crystal analysis. Thermal stabilities and decompositions of the complexes were examined under inert nitrogen atmosphere. The antifungal, antibacterial and anticancer activities were also tested using three plant pathogens (*Alternaria solani*, *Rhizoctonia solani* and *Fusarium oxysporum*), ten bacteria (*E. coli*, *P. aeruginosa*, *S. enteritidis*, *P. vulgaris*, *K. pneumonia*, *S. aureus*, *E. faecalis*, *B. subtilis*, *B. cereus* and *C. albicans*) and four cancer cells (*HT29, HeLa, C6, and Vero cell lines*), respectively.

Description of the Crystal Structures

The **C3**, **C4** and **C5** crystallize in an I2/a space group. The crystal structures of **C3**, **C4** and **C5** are illustrated in Figure 1a, 1b and 1c, while the selected bond lengths and angles are given in Table 1-3, respectively. The asymmetric complex unit formed out of three metal centred $[Cu(hydeten)_2Au_2(CN)_4].CH_3OH$ (**C3**), $[Zn(hydeten)_2Au_2(CN)_4].H_2O$ (**C4**), and $[Cd(hydeten)_2Au_2(CN)_4].H_2O$ (**C5**).

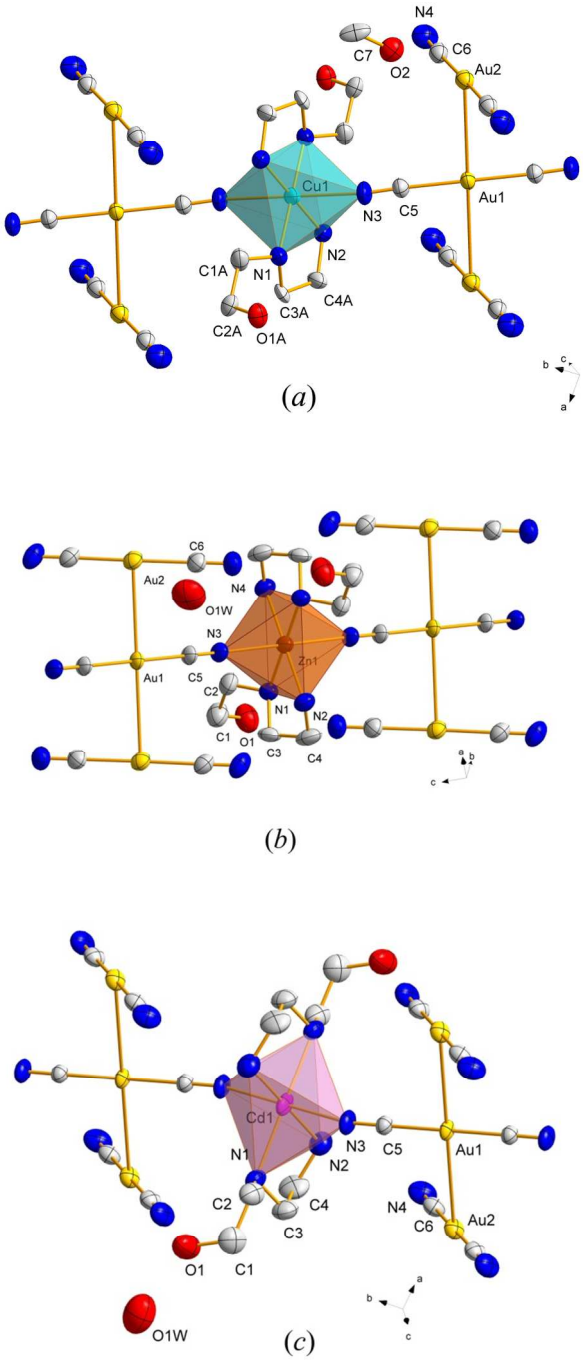

Fig 1. Atom labelled scheme and polyhedral representation of **C3** *(a)*, **C4** *(b)* and **C5** *(c)*. Asymmetric unit is formed by the named atoms. H atoms omitted for clarity.

The asymmetric units are linked to each other via –CN–M(hydeten)–NC–Au(1)–CN–M(hydeten)–CN– chains (M= Cu^{II}, Zn^{II} and Cd^{II}) and aurophilic interacted –Au(1)(CN)2–Au(2)(CN)2–Au(1)(CN)2–Au(2)(CN)2– zig-zag shaped chains along the *a* axis (Fig. 2a). The chains are crossed over Au(1) and the packing results in *3D* formation. Interestingly, within the *3D* network, these two interpenetrating nets are supported by Au···Au aurophilic interactions (Fig. 2b). The aurophilic (Au···Au) interactions in the crystal structures of gold compounds, as well as in solution, has fascinated chemists for decades.[41-45] One of the reasons for this interest is that the formation of Au···Au interactions has been employed in the analytical detection of chemical species,"chemo-sensing"[46] and recently utilised to monitor the formation of coordination polymers.[47] Aurophilic interactions can also lead to fascinating supramolecular architectures.[48-50]

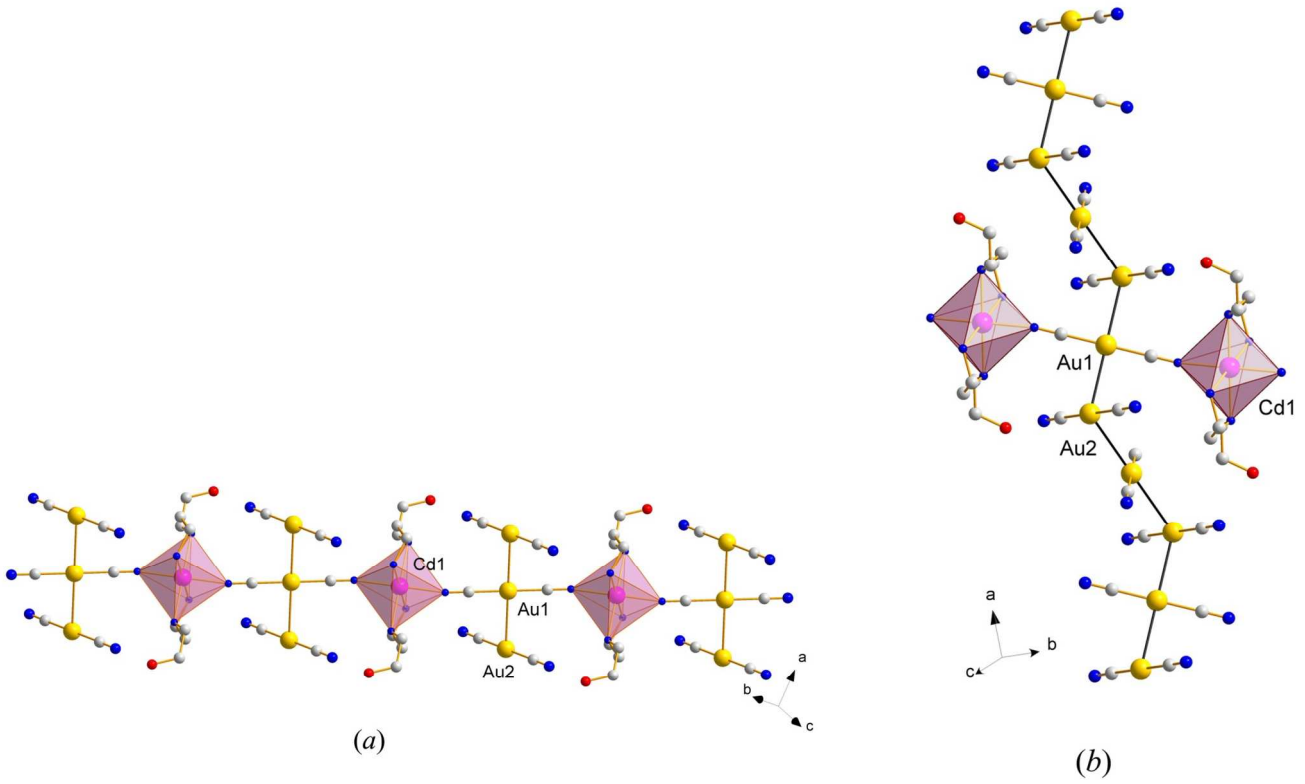

Fig 2. Representation of –CN–Cd(*hydeten*)–NC–Au(1)–CN–Cd(*hydeten*)–CN– chain for **C5** *(a)* and Au···Au aurophilic interactions in **C5** running along *a* axis *(b)*. H atoms and lattice water oxygens omitted for clarity.

While the Au(1)–Au(2)–Au(1)^{ii} angles of the **C3**, **C4** and **C5** are 131.73(2)º, 119.75(2)º and 120.77(2)º along the zig-zag shaped chain, their Au(1)–Au(2) distances are 3.193(3), 3.149(2) and 3.193(2) Å respectively. The angle around the $Au^{I}(CN)_2$ centres, that act as bridges between M^{II}(*hydeten*) (M^{II}=Cu, Zn and Cd), are exactly linear with the bond angle C(5)–Au(1)–C(5)^{i} and Au(2)– Au(1)–Au(2)^{ii} of 180º. Also, the intramolecular M...Au distances are Cu(1)...Au(1): 5.450 (4) Å; Cu(1)...Au(2): 6.690(4) Å, Zn(1)...Au(1): 5.312 (4) Å; Zn(1)...Au(2): 6.215(4) Å and Cd(1)...Au(1): 5.4864(4) Å; Cd(1)...Au(2): 6.210 (4) Å. Combining of these rings, 12 metal centred and 20 membered rings occurs in the crystal packing of the complexes (Fig. 3).

Table 1 Selected bond lengths (Å) and angles (º) for **C3**

Bond lengths			
Au1–Au2	3.1931(3)	N1–C3A	1.465(14)
Au1–C5	2.007(10)	N1–C4A	1.471(17)
Au1–C6	1.987(14)	N3–C5	1.094(14)
Cu1–N1	2.052(9)	N4–C6	1.159(18)
Cu1–N2	1.986(10)	C7-O2	1.38(3)
N1–C1A	1.506(17)		

Bond angles[a]			
Au2[1]—Au1—Au2	180.0	C6[2]—Au2—Au1[2]	97.0 (3)
C5—Au1—Au2[1]	85.0 (3)	C6—Au2—C6[2]	177.3 (6)
C5—Au1—Au2	95.0 (3)		
Au1—Au2—Au1[2]	131.73 (2)		
C6—Au2—Au1	97.0 (3)		
C6—Au2—Au1[2]	84.1 (3)		

[a] [1]-x+2,-y,-z; [2]3/2-x,+y,-z

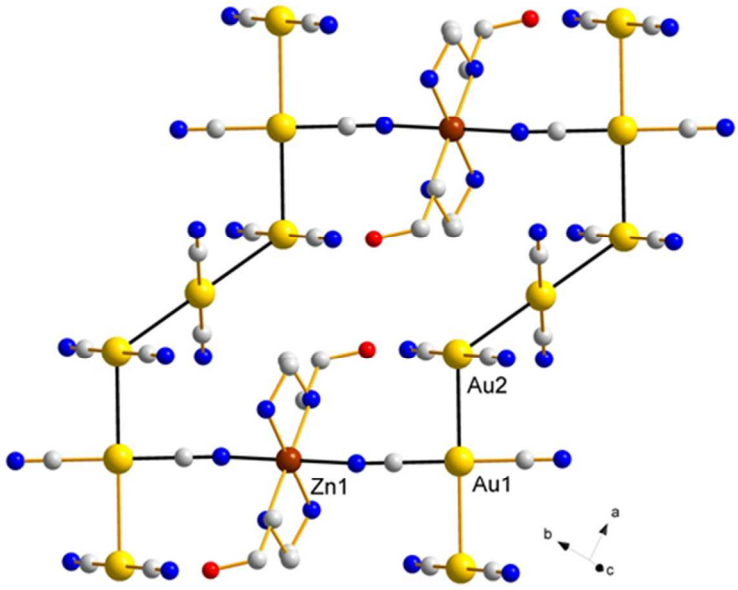

Fig 3. 12 Metal centered ring occurs by the combining of two chains.

X-ray data of [Cd(*hydeten*)$_2$Au$_2$(CN)$_4$].H$_2$O (**C5**) indicate that the environment around the Cd^{II} atom, settled in the symmetry centre, has the square–bipyramidal geometry. The basal plane occupied by the four N atoms from the *hydeten* ligand. The equatorial plane is planar. The five membered backbone *hydeten* ring (Cd–N1–C3–C4–N2) has twisted envelope conformation. The puckering parameters are q_2=0.543(2) Å and φ_2= 271.0(12)º. The puckering parameters q_2 and φ_2, relate to the deviations of the atoms from the mean plane of the ring, should be compared to the ideal values of q2>0 and φ_2=0 for the envelope conformation versus q_2>0 and φ_2=90 for the twisted conformation.[51] The other

metal coordinated N atoms of $Au(CN)_2$ lies in the axial positions. While the Cd–$N_{hydeten}$ bond lengths are equal to 2.322(9) and 2.336(10) Å, respectively, the Cd– $N_{Au(CN)2}$ bond length is 2.329 Å. The linear bond angles around Cd^{II} ion do not deviate from 180º.

Table 2 Selected bond lengths (Å) and angles (º) for **C4**

Bond lengths[a]			
Zn1–N1	2.191(7)	N4–C6	1.135(11)
Zn1–N3[1]	2.212(6)	Au1–Au2	3.1491(3)
Zn1–N2	2.139(7)	Au2–Au1[2]	3.1490(3)
Zn1–N3	2.212(6)	Au1–C5	1.993(6)
N3–C5	1.134(9)	Au2–C6	1.991(12)
Bond angles[b]			
N1[1]–Zn1–N1	180.0(1)	Au2-Au1-Au2[2]	180.0
N1–Zn1–N3[1]	89.5(3)	Au1[3]-Au2-Au1	119.751(15)
N1[1]–Zn1–N3[1]	90.5(3)	C5[2]-Au1-Au2	88.1(2)
N1–Zn1–N2[3]	90.5(3)	C5-Au1-Au2	91.9(2)
N2–Zn1–N1	82.3(3)	C6[3]-Au2-Au1	92.9(2)
N2[1]–Zn1–N1	97.7(3)	C6-Au2-Au1	87.7(3)
N2–Zn1–N2[1]	180.0(1)	C6[3]-Au2-C6	178.7(5)

[a] [1]-1/2-x,1/2-y,1/2-z; [2]1/2-x,+y,1-z; [b] [1]2-x,-y,-z; [2]3/2-x,+y,-z; [3]5/2-x,1/2-y,1/2-z

Table 3 Selected bond lengths (Å) and angles (º) for **C5**

Bond lengths[a]			
Cd1–N1	2.336(9)	Au1–Au2	3.1718(4)
Cd1–N2	2.322(11)	Au2–Au1[1]	3.1719(4)
Cd1–N3	2.329(9)	Au1–C5	1.962(10)
N3–C5	1.173(13)	Au2–C6	2.001(9)
N4–C6	1.161(15)		
Bond angles[b]			
N1–Cd1–N1[1]	180.0	Au2[2]-Au1-Au2	180.0
N2[1]–Cd1–N1[1]	78.2(4)	Au1-Au2-Au1[3]	120.77(2)
N2–Cd1–N1[1]	101.8(4)	C5[2]-Au1-Au2	92.0(3)
N2–Cd1–N2[1]	180.0(3)	C5-Au1-Au2	88.0(3)
N2[1]–Cd1–N3[1]	88.7(4)	C6[3]-Au2-Au1	86.4(3)
N2–Cd1–N3[1]	91.3(4)	C6-Au2-Au1	94.0(3)
N3–Cd1–N1	90.3(4)	C6[3]-Au2-C6	179.2(8)
N3[1]–Cd1–N1	89.7(4)		

[a] [1]3/2-x,+y,1-z; [b] [1]:3/2-x,-1/2-y,1/2-z; [2]:2-x,-1-y,1-z; [3]: 3/2-x,+y,1-z

The environment around the $[Zn(hydeten)_2Au_2(CN)_4].H_2O$ (**C4**) has the same coordination with **C5**. *Hydeten* coordinate to the metal centre as five membered chelate as in **C5** and Zn–N1–C3–C4–N2 ring has twisted envelope conformation with the q_2=0.484(1) Å and φ_2= 271.3(8)º

puckering parameters. While the Zn–$N_{hydeten}$ bond lengths are equal to 2.191(9) and 2.139(10) Å, respectively, the Zn–$N_{Au(CN)2}$ axial bond length is 2.212 Å. All the Zn–N bond lengths are shorter than the related bond lengths in **C5**. Meanwhile, the linear bond angles around Zn^{II} ion do not deviate from 180º as in **C5**.

While the Cu^{II}(*hydeten*) centers coordinates to two nitrile nitrogen atoms from two terminal $Au^{II}(CN)_2$ ligands in axial position as in the **C4** and **C5**, the Cu–N_{axial} distance much longer than the other examined complexes. Glancing Table 1, it is observed that the dominant impact of Jahn-Teller effect in complex **C3**. The basal plane around the symmetry centred Cu completed by the four N atoms from the *hydeten* ligand. The N The equatorial plane is planar like the other structures. Just here, it should be emphasized that the Cu–$N_{hydeten}$ bond lengths are shorter than the other synthesized complexes. It can be said that the cause of bond shortening is Jahn-Teller effect. The five membered backbone *hydeten* ring (Cu–N1–C3–C4–N2) has again twisted envelope conformation as in the **C4** and **C5**. The puckering parameters are q_2=0.3987(2) Å and φ_2= 85.7304 (12)º. The linear bond angle around Cu^{II} ion is equal to 180º as in **C4** and **C5**.

The results presented herein show that weak *H*-bonds interactions and the rather distinctive organizing forces, such as aurophilic interactions, can be successfully employed to design crystal packing and *3D* architectures. In addition to aurophilic the interaction, O–H...Ow and N–H...N type H-bond interaction of **C5** plays an important role in *3D* crystal packing with the summarized parameters in Table 4. It should be pointed that it is not possible the placement of the hydrogen atoms for O1W, because of the O1W placed on symmetry centre. Unlike the **C5**, the Ow–H...O, O–H...N and N–H...N -type H-bonds in **C4** provide an additional contribution to *3D* packing as summarized in Table 4. Especially, water and *hydeten* oxygen's contribute to the H-bond as donor atoms with the O1w...O1:2.776Å, O1...N4:2.871 Å relatively short bond lengths (Fig. 4).

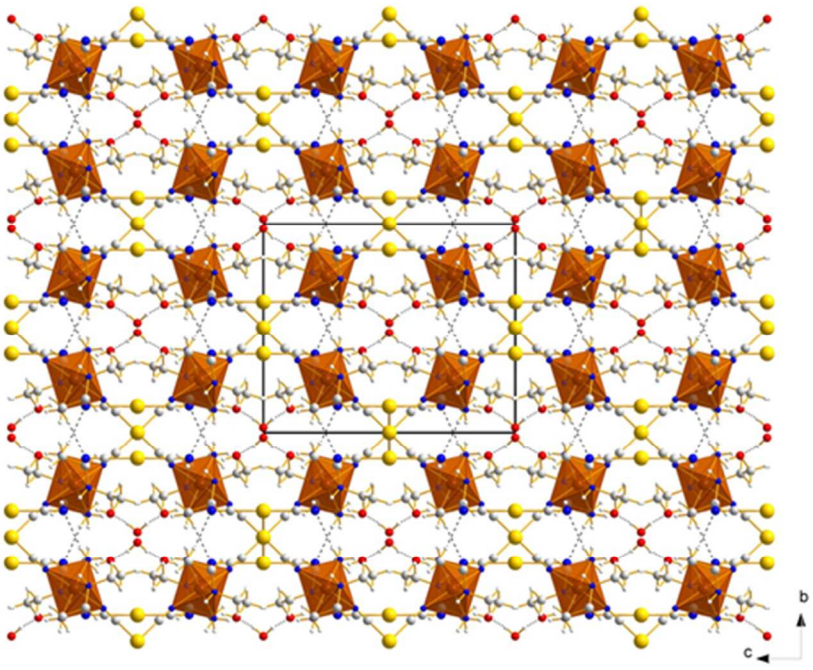

Fig 4. Packing diagram and *H*-Bonds interactions of **C4**. Aqua coloured polyhedrons represent the coordination around Zn.

Table 4 Hydrogen bonds for **C3**, **C4** and **C5**

D–H···A	*D–H (Å)*	*H···A (Å)*	*D···A (Å)*	*D–H···A (°)*
C3[a]				
N2—H2*BD*···O1*A*[1]	0.90	2.08	2.97(2)	174
O1*A*—H1*AA*···O2[2]	0.82	2.12	2.91(3)	162
O1*B*—H1*BA*···N1	0.82	2.24	2.71(2)	117
O1*B*—H1*BA*···O1*B*[3]	0.82	2.42	2.92(4)	121
C7—H7*A*···O1*A*[4]	0.96	2.05	2.78(3)	132
C7—H7*B*···N4[5]	0.96	2.09	2.71(3)	121
O2—H2···N4[5]	0.82	2.35	2.89(2)	124
C4[b]				
N1–H1A···N4[1]	0.91	2.40	3.23(1)	151.7
N2–H2D···N4[2]	0.90	2.53	3.34(1)	150.9
O1–H1C···N4[1]	0.82	2.08	2.87(1)	161.1
O1W–H1W···O1[3]	0.83	2.04	2.77(1)	148.2
C5[c]				
N1–H1···N4[1]	0.91	2.34	3.20(2)	157.2
N2–H2D···N4	0.90	2.43	3.28(2)	156.0
O1–H1C···O1W	0.82	2.05	2.76(1)	145.6

[a] [1] *x, −y+1/2, z+1/2;* [2] *x+1, y, z;* [3] *−x+5/2, y, −z;* [4] *x−1, y,−z;* [5] *x, − y+1/2, z−1/2*
[b] [1] *-1/2-x,1/2-y,1/2-z;* [2] *-1/2+x,-y,+z;* [3] *-1-x,1-y,1-z;* [c] [1] *-1-x,1/2+y,1/2-z*

Unlike other complexes, the asymmetric unit of **C3** consist of guest methanol solvent in the crystal packing. Because of this reason, there are differences in the H-bonding interactions from the other structures. The $N_{hydeten}$...$N_{nitrile}$, C_{meth}...$N_{nitrile}$ and $N_{hydeten}$...O-type H-bonds provide an additional contribution to *3D* packing as summarized in Table 3. In contrast to other studied structures, the *3D* structure of **C3** consists of cavities (Fig. 5). The void volume V_{void} is 8.4% of the total crystal volume (2214.4Å^3), as calculated using the Platon program.[52] The solvent-accessible volume of the cavity is 186.1Å^3, which includes methanol molecules.

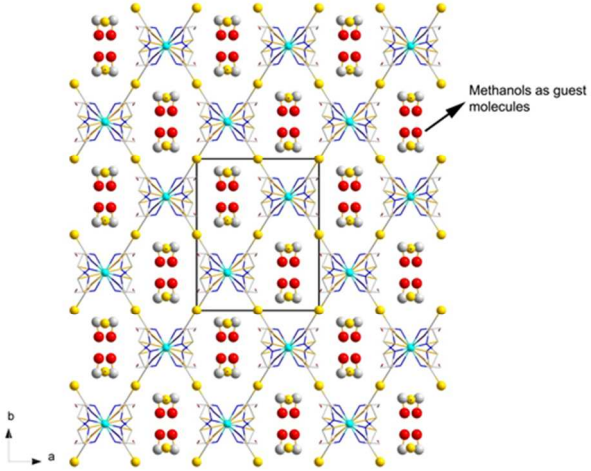

Fig 5. Crystal packing scheme and representation of cavities. Cavities filled by the guest methanol molecules. H atoms omitted for clarity.

Thermal Properties of the complexes

Thermal analysis data obtained under nitrogen atmosphere showed that all of the complexes exhibited similar thermal behaviors. Thermal decomposition of **C1** and **C2** occurred at three and six intermediate steps respectively, while thermal decomposition of **C3**, **C4,** and **C5** took place in four intermediate steps (Table 5). When compared with the thermal stability of the complexes it is revealed that **C1** (213 ºC) is the most thermally stable as **C2** is the second one (196 ºC). The other three complexes (**C3**, **C4**, and **C5**) are found to be stable up to 101, 115, and 128 ºC respectively as shown in Table 5.

Table 5 tabulated the thermal data of the complexes in detail also. The first step decomposition was assigned to delivery of crystal water of **C2**, **C4**, and **C5**; and methanol of **C3** in the lattice. The first step decomposition of the crystal water-free **C1** and the second step decomposition of the rest of the complexes released the neutral ligand *hydeten*, as expected. While the thermal decomposition of *hydeten* of **C1**, **C3,** and **C5** complexes took place in one step, that of **C2** and **C4** occurred in three steps. Following decomposition steps were found to be due to cyanido groups evolution except for **C3** cyanide groups of that started to disappear in the second step and completed then. At the final step, decomposition of the complexes resulted in the formation of NiO+2Au (for **C1** and **C2**), Cu+2Au (for **C3**), ZnO+2Au (for **C4**) and 0.7Cd+2Au (for **C5**).

Table 5 Thermoanalytical data of the complexes

Complex	Stage	Temperature Range (°C)	DTG_{max}	Mass Loss Δm (%)		Total Mass Loss Δm (%)		Liberated Group and Residue
				Found	Calcd.	Found	Calcd.	
$[Ni(hydeten)Au_2(CN)_4]$ (**C1**)	1	213-310	268	15.44		15.44	15.76	*hydeten*
	2	310-383	327	6.20				
MW: 660.84 g/mol	3	383-510	419	7.96		29.60	29.07	4CN
						70.40	70.93	NiO+2Au
$[Ni(hydeten)_2Au_2(CN)_4].H_2O$ (**C2**)	1	43-117	85	2.10		2.10	2.30	H_2O
	2	196-223	217	2.68				
	3	223-274	242	12.46				
	4	274-413	315	9.61	26.60	26.85	28.90	~2*hydeten*
MW: 783.01 g/mol	5	413-498	466	4.86				
	6	498-619	532	8.09		39.80	40.13	4CN
						60.20	59.87	NiO+2Au
$[Cu(hydeten)_2Au_2(CN)_4].CH_3OH$ (**C3**)	1	35-101	72	3.99		3.99	3.99	CH_3OH
	2	101-308	232	29.75	29.47	33.74	33.46	2*hydeten* +CN
	3	308-424	343	3.76				
MW: 801.91 g/mol	4	424-959	573	5.54		43.04	42.92	3CN
						56.96	57.08	Cu+2Au
$[Zn(hydeten)_2Au_2(CN)_4].H_2O$ (**C4**)	1	35-115	85	2,14		2.14	2.27	H_2O
	2	115-263	221	12,41	13.19	14.55	15.46	*hydeten*
	3	263-463	278	10,60				
MW: 789.71 g/mol	4	463-887	557	14,06	24.37	39.21	39.81	*hydeten* + 4CN
						60.79	60.22	ZnO+2Au
$[Cd(hydeten)_2Au_2(CN)_4].H_2O$ (**C5**)	1	35-119	74	1.94		1.94	2.15	H_2O
	2	128-418	233	24.72	24,89	26.66	27.04	*2hydeten*
	3	418-746	654	10.40		37.06	36.36	3CN
MW: 836.74 g/mol	4	835-1064	1007	7.10		44.16	43.49	CN + 0,3Cd
						55.84	56.51	0.7Cd+2Au

Biological Activities

Antifungal activities of the complexes

The antifungal activities of **C1**, **C2**, **C3**, **C4** and **C5** obtained by the well diffusion method, are shown in Table 6. The effectiveness of the compounds varies according to the fungus species. **C1**, **C2** and **C4** showed significant inhibitory effect on fungal growth against all test fungi at all doses tested, while **C3** and **C5** had no fungicidal effects on *A. solani* and *R. solani* even at higher dose (20 µg/mL) (Table 6). **C2** was more effective antifungal agent than **C1**, **C3**, **C4** and **C5** against A. solani, followed by *R.solani* and *F. oxysporum* (Table 6). Compared with the antifungal activity of gold based compounds tested in the present study, the silver based compound, tested in previous study, had better activity against *A. solani* and *R. solani* and the inhibitory indices of $[Ni(hydeten)_2Ag(CN)_2]$ $[Ag(CN)_2].H_2O$ and $[Cd_2(hydeten)_2Ag_4(CN)_8]$ are 88.38% 83.27% against *A.solani* and 75.95% 75.12% against *R. solani* at 20 µg/mL dose, respectively.[39] It is obvious that silver based compounds show much better antifungal activity due to the introduction of silver. With **C1** zone of inhibition was maximum against *F. oxysporum* subsequently followed by *R. solani* and *A. solani*. The results indicated that all the *hydeten* compounds were significantly reduced the mycelial growth of the *F. oxysporum* at all concentrations. An enhancement in antifungal activity against F. *oxysporum* was observed, with increase in concentration of the chemicals (Table 6). Efficacy of the compounds when compared with two fungicides such as Copper hydroxide and Maneb revealed that, Copper hydroxide inhibited mycelial growth of *A. solani* but inhibition of mycelial growth by **C2** was much more than Copper hydroxide. Effective inhibition of mycelial growth in *F. oxysporum* was significant by all the tested chemicals as compared to Maneb. The calculated LC50 values of the **C1** and **C4** against mycelial growth of *A.solani* is shown in Table 7. The LC50 of the inhibition of **C1** and **C4** against mycelial growth of *A. solani* were 11.164 µg/mL and 14.683 µg/mL respectively. Besides, the LC50 of the inhibition of C1a against mycelial growth of R. solani was 12.105 µg/mL (Table 7). In addition, the LC50 of the inhibition of **C1**, **C2**, **C3**, **C4** and **C5** against *F. oxysporum* were 5.416, 17.843, 7.127, and 11.914 µg/mL respectively (Table 7). The lowest LC50 value of 5.416µg/mL was obtained with **C1** against *F. oxysporum*, followed by **C4** with 7.127 µg/mL. For the first time, the effectiveness of these complexes according to growth inhibition of above mentioned fungi is reported. In conclusion, the findings of this study confirmed that the compounds may be used with relative safety for control of various plant pathogens fungi, compared to synthetic fungicides. Moreover, this report opens up for further research, the area of mode of action of the complexes.

Table 6 Antifugal activities of the complexes against plant pathogenic fungi

Dose(µg/mL)	Complexes/Growth inhibition (%)				
	C1	**C2**	**C3**	**C4**	**C5**
	Alternaria solani				
20.0	65,8[a*]	81,9[a]	0,0	62,9[a]	0,0
15.0	50,2[b]	79,0[ab]	0,0	47,8[b]	0,0
10.0	44,6[bc]	76,2[bc]	0,0	44,4[c]	0,0
7.5	38,9[c]	72,6[cd]	0,0	27,4[d]	0,0
5.0	30,1[d]	70,4[d]	0,0	21,3[e]	0,0
$Cu(OH)_2$	68,0a	68,0[a]	68,0	68,0[a]	68,0
DMSO	0,0[e]	0,0[e]	0,0	0,0[f]	0,0
LSD	6,8	5,4		5,4	
	Rhizoctonia solani				

20.0	67,5[a*]	51,3[a]	0,0	48,2[a]	0,0
15.0	49,8[b]	29,0[b]	0,0	41,6[ab]	0,0
10.0	43,7[c]	15,2[c]	0,0	38,4[b]	0,0
7.5	38,0[c]	0,0[d]	0,0	37,5[b]	0,0
5.0	15,1[d]	0,0[d]	0,0	35,2$_b$	0,0
$Cu(OH)_2$	0,0[e]	0,0[d]	0,0	0,0$_c$	0,0
DMSO	0,0[e]	0,0[d]	0,0	0,0[c]	0,0
LSD	6,0	2,5		8,1	
	Fusarium oxysporum f.sp. *lycopersici*				
20.0	75,0[a*]	48,0[b]	69,2[a]	73,3[a]	48,4[b]
15.0	75,3[a]	44,9[bc]	42,2[c]	59,6[b]	36,0[c]
10.0	65,0[b]	38,1[cd]	28,6[d]	51,9[cd]	30,4[d]
7.5	54,8[c]	35,9[d]	23,4[d]	51,5[cd]	26,8[de]
5.0	44,8[d]	18,9e	13,5[e]	48,3[d]	23,5[e]
Maneb	56,3[c]	56,3[a]	56,3[b]	56,3[bc]	56,3[a]
DMSO	0,0[e]	0,0[f]	0,0[f]	0,0[e]	0,0[f]
LSD	6,6	7,5	7,5	5,7	5,3

*Means in a column followed by the same letter are not significantly different (ANOVA, P < 0.05)

Table 7 Summary of probit analysis parameters from the dose-response test

Complex	Slope (±SE)[a]	LC50 (95% of fiducial limits)	$\chi 2^b$
	Alternaria solani		
C1	1.154±0.392	11.164(8.476-15.652)	2.154
C3	1.738±0.402	14.683(11.727-21.648)	1.699
	Rhizoctonia solani		
C1	2.091±0.408	12.105(10.087-15.238)	3.03
	Fusarium oxysporum f.sp. *lycopersici*		
C1	1.320±0.397	5.416(2.053-7.529)	1.188
C2	1.38±0.399	17.843(13.208-39.399)	2.117
C4	1.099±0.389	7.127(2.680-9.986)	2.683
C5	2.073±0.405	11.914(9.912-14.996)	5.041

[a]Slope of the concentration (±standard error) response of the fungi to complexes
[b]Pearson chi-square goodness-of-fit test on the probit model (α=0.05)

Antibacterial activities of the complexes

Agar plate dilution test was used to determine the Minimum Inhibitory Concentration (MIC) of the antibacterial complexes. The technique involves the incorporation of different concentrations of the antibacterial substance into a nutrient agar medium followed by the application of a standardized number of cells to the surface of the agar plate. In present study standardized numbers of reference microorganism cells were inoculated onto plates by surface spread plate method and the test compounds were spotted on the inoculated plates. After appropriate incubation time, inhibition zone were produced by each compound and the lowest concentration at which there is no visible zone of inhibition was taken as the MIC. The experiment was repeated three times and the arithmetic mean of the MIC values are given in Table 8. As it was seen in Table 8, **C3** was higher inhibitory effect against gram (+) bacteria than gram (-) bacteria except *E.coli* ATCC 11229. Interestingly **C3** is highly antibacterial against gram negative virulent *E.coli* ATCC 11229.

According to the spot on lawn method the antibacterial activity of the compounds were determined by measuring the halo zones around the *hydeten* compounds (5 µg). The size of the inhibition zones for *E. coli* ATCC 11229 were in the following order: **C3** (38 mm) > **C5** (34 mm)

>Amp (33 mm) > **C2** (29 mm) > **C1** (27 mm) > **C4** (24 mm) > KCN (0 mm) =DMSO (0 mm). The halo zones of inhibition for B. cereus DSM4312 was lower than *E.coli* except for **C5**. [**C5** (35 mm)> **C3** (34 mm) > **C2** (19 mm) > **C1** (18 mm) = **C4** (18 mm) > DMSO (10 mm) > Amp (8.6 mm)]. According to Table 8, it was obvious that **C1** and **C2** were more active against gram negative bacteria than gram positive bacteria. But it was not seen significant activity against the yeast *C. albicans*.

As a result, it is obvious that **C3** and **C5** have promising activity for future works. In general, *hydeten* complexes with dicyanidoaurate(I) which were synthesized in this work had higher activity than dicyanidoarjentate(I)-*hydeten* compounds in our previous work.[39] Especially **C2** were more active against *E.coli* than its silver conjugate. It was also obvious that $[Cu^{II}(hydeten)][Au^{I}(CN)_2]_2 \cdot CH_3OH$ (**C3**) had the highest activity. It is known that because of the inherent elemental properties of silver, it has strong antibacterial activity, but when the gold was modified by other elements like Cu^{II} (**C3**) or Cd^{II} (**C5**), its antimicrobial activity was increased.

Table 8 Minimum inhibitory concentrations of the complexes

Strains	MIC (mg/L)				
	C1	**C2**	**C3**	**C4**	**C5**
E. coli ATCC 11229	500	500	62,5	1000	62,5
*P. aeruginosa*ATCC29213	250	250	≥2000	250	2000
*S. enteritidis*ATCC13076	250	250	500	250	500
P. vulgaris Kuen1329	250	250	≥2000	250	1000
K. pneumonia ATCC700603	≥2000	≥2000	≥2000	≥2000	1000
*S. aureus*ATCC 25213	≥2000	1000	500	1000	500
*E. faecalis*ATCC51299	1000	1000	250	1000	500
*B. subtilis*ATCC6633	500	≥2000	1000	500	1000
B. cereus DSM4312	1000	1000	62,5	1000	62,5
*C. albicans*ATCC1223	1000	1000	≥2000	1000	1000

Anticancer activities of the complexes

Many anticancer drug candidates did failure clinical trials or have been withdrawn from pipeline because of serious side effects, loss of sensitivity to drugs, and limited use for many tumor types. Research efforts are focused on developing novel anti-tumor drugs to ameliorate clinical effectiveness and to minimize general toxicity and drug resistance. Silver and gold complexes are found to be promising alternatives to old anti-cancer agents, showing activity on tumors that have developed resistance. The serious limitations of cancer treatments have prompted many researchers to develop alternative strategies based on different metals, ligands, and mechanisms for cancer. Transition metal complexes of this type have not been extensively explored for their chemotherapeutic usage. In the present study, **C1**, **C2**, **C3**, **C4** and **C5** were synthesized and tested for their anticancer and cytotoxic activities against *C6* (rat brain tumor), HeLa (human cervical cancer), HT29 (human colon cancer), and Vero (African green monkey kidney) cell lines. These compounds exhibited very high anti-proliferative effects on cancer cells according to the test results.

I. Antiproliferative effect of **C1**, **C2**, **C3**, **C4** *and* **C5**

The anticancer activities of the complexes, $[Au(CN)_2]^-$ and 5FU against HT29, HeLa, *C6*, and Vero cell lines were determined using a BrdU cell proliferation ELISA (Fig. 6). $[Au(CN)_2]^-$ was the most antiproliferative compound tested on all cell lines ($P < 0.05$), but it was found to be significantly toxic to the cells at concentrations of 0.2 µg/mL and higher (Fig. 6). $[Au(CN)_2]^-$ was necrotic to cells, which may lead to rapid cell-membrane disintegration. **C1, C2, C3, C4** and **C5** showed significantly ($P<0.05$) higher antiproliferative activity than 5FU against the cancer cell lines tested. Moreover, test compounds displayed apoptotic activity rather than necrotic to cells. The data from the experiments suggest that the IC_{50} concentrations of test compounds, $[Au(CN)_2]^-$, and 5FU were 0.26, 0.22, 0.27, 0.28, 0.14, 0.10 and 35.86 µg/mL for HeLa; 0.20, 0.18, 0.18, 0.19, 0.13, 0.11 and 28.29 µg/mL for *C6*; 0.34, 0.30, 0.29, 0.38, 0.13, 0.12 and 33.62 µg/mL for HT29; and 0.33, 0.36, 0.31, 0.24, 0.23, 0.13 and 35.42 µg/mL for Vero, respectively.

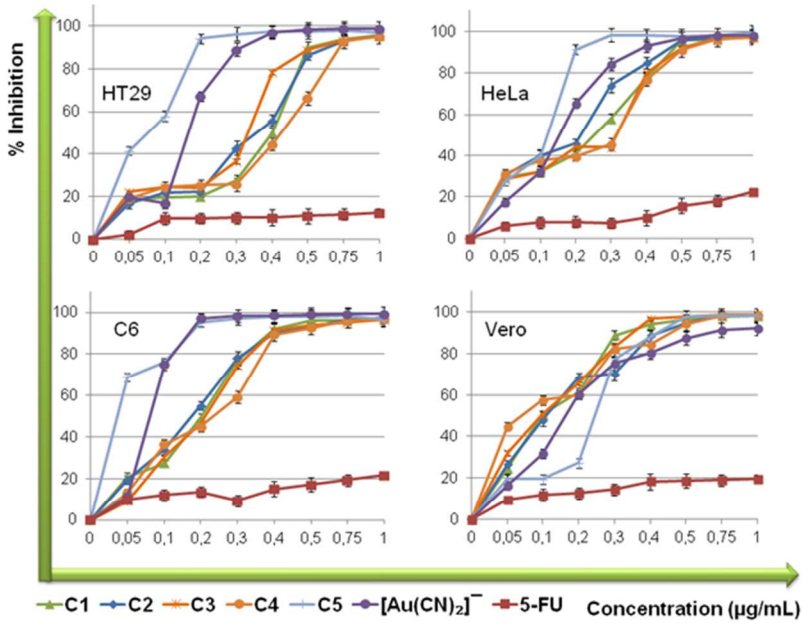

Fig 6. Effects of test compounds and $[Au(CN)_2]^{1-}$ on the proliferation of HT29, HeLa, *C6* and Vero cell lines. Exponentially growing cells were incubated with **C1, C2, C3, C4** and **C5** and $[Au(CN)_2]^{1-}$ for 24 hours and the cell proliferation was measured by the BrdU Cell Elisa assay. Percent inhibition was reported as mean values ± SEM of three independent assays.

II. Cytotoxic activity of **C1**, **C2**, **C3**, **C4**, **C5**, *$[Au(CN)_2]^{1-}$ and 5FU*

The cytotoxic activities of test compounds, $[Au(CN)_2]^-$ and 5FU on HeLa, HT29, *C6*, and Vero cell lines were tested using an LDH cytotoxicity assay kit. In contrast to the high cytotoxicity of the ligand on the cell lines, the cytotoxicities of **C1**, **C2**, **C3**, **C4** and **C5** were close to the cytotoxicity of 5FU at their IC_{50} concentrations (Fig. 7). The percent cytotoxicity of test compounds, and 5FU ranged from 15% to 25%, whereas $[Au(CN)_2]^-$ showed about 60% cytotoxicity ($P < 0.05$) against all cell lines (Fig. 7). Therefore, it is suggested that these compounds may have cytostatic potential rather than cytotoxic potential. The significantly lower cytotoxicity of **C1**, **C2**, **C3**, **C4** and **C5** than

$[Au(CN)_2]^-$ alone may indicate that the cytotoxicity of $[Au(CN)_2]^-$ decreases to cytotoxicity levels of 5FU when complexed with *N*-(2-hydroxyethyl)-ethylenediamine *(hydeten)* in test compounds without reducing their antiproliferative potential.

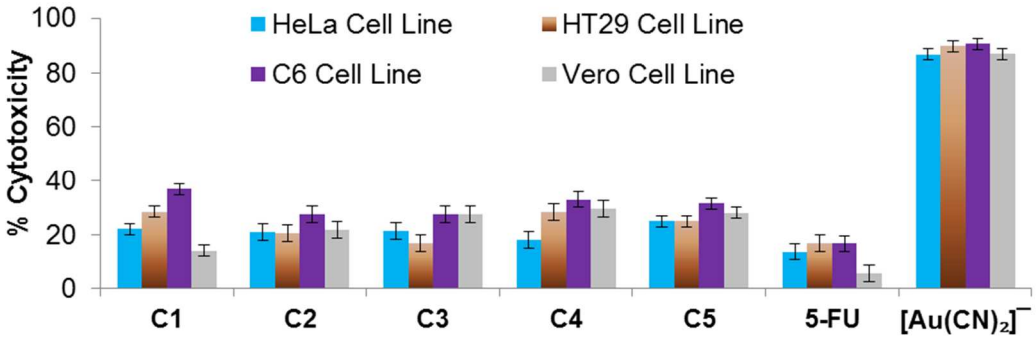

Fig 7. Cytotoxic activity of test compounds, and $[Au(CN)_2]^{1-}$ on HT-29, HeLa, *C6* and Vero cell lines. Exponentially growing cells were incubated with IC_{50} concentrations of test compounds, and $[Ag(CN)_2]^{1-}$ and cytotoxicity was determined by LDH Cytotoxicity Assay. Cytotoxicity of **C1**, **C2**, **C3**, **C4** and **C5** was siginificantly ($p < 0.05$) lower than $[Au(CN)_2]^{1-}$. Percent cytotoxicity was reported as mean values ± SDs of three independent assays.

III. Detection of apoptotic potential of **C1**, **C2**, **C3**, **C4** *and* **C5** *by DNA laddering Assay*

In the present study, to test whether the mechanism of antiproliferative and cytotoxic activity of test compounds involves apoptosis, we determined DNA laddering potential of **C1**, **C2**, **C3**, **C4** and **C5** on HeLa, HT29 and *C6* cell lines. The DNA laddering assay results showed that all coordination compounds tested caused fragmentation of DNA, indicating that these compounds act by inducing apoptosis (Fig. 8). These results were parallel to antiproliferative and cytotoxic activities test compounds.

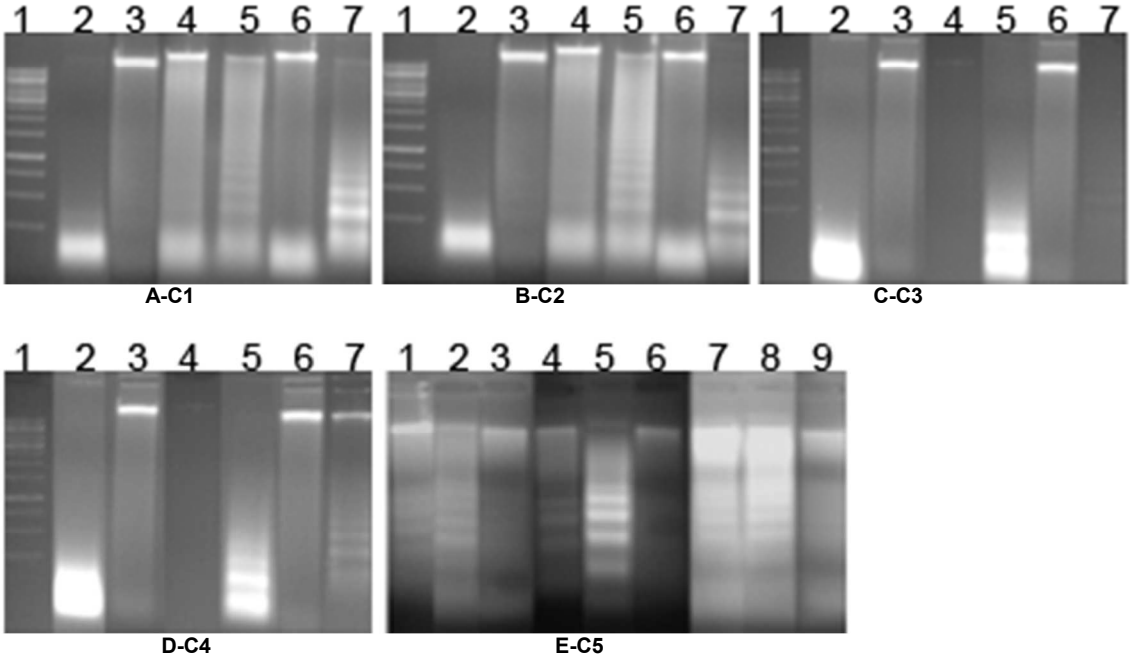

Fig 8. Effects of **C1**, **C2**, **C3**, **C4** and **C5** on DNA fragmentation. All the test compounds were caused DNA fragmentation. (A-**C1**: Lane 1, DNA standard; Lane 2, HeLa+**C1**; Lane 3, HeLa Control; Lane 4, HT29 Control; Lane 5, HT29+**C1**; Lane 6, *C6* Control; Lane 7, *C6*+**C1**. B-**C2**: Lane 1, DNA standard; Lane 2, HeLa+**C2**; Lane 3, HeLa Control; Lane 4, HT29 Control; Lane 5, HT29+**C2**; Lane 6, *C6* Control; Lane 7,

C6+**C2**. C-**C3**: Lane 1, DNA standard; Lane 2, HeLa+**C3**; Lane 3, HeLa Control; Lane 4, HT29 Control; Lane 5, HT29+**C3**; Lane 6, *C6* Control; Lane 7, C6+**C3**. D-C4: Lane 1, DNA standard; Lane 2, HeLa+**C4**; Lane 3, HeLa Control; Lane 4, HT29 Control; Lane 5, HT29+**C4**; Lane 6, *C6* Control; Lane 7, *C6*+**C4**. E-C5: Lane 1, *C6*+Camptothecin; Lane 2, *C6*+**C5**; Lane 3, *C6* Control; Lane 4, HT29+Camptothecin; Lane 5, HT29+**C5**; Lane 6, HT29 Control; Lane 7, HeLa+Camptothecin; Lane 8, HeLa+**C5**; Lane 9, HeLa Control).

IV. Detection of apoptotic potential of **C1**, **C2**, **C3**, **C4**, *and* **C5** *by TUNEL assay*

The apoptotic potential of test compounds on HT29 cell lines was tested further by TUNEL assay. As shown in Figure 9, test compounds and DNase I (PC, positive control) treated cells showed green fluorescence, indicating the fragmented DNA in apoptotic cells (**C1**, **C2**, **C3**, **C4**, **C5**, and **PC**), whereas the DMSO control was TUNEL-negative (NC). The TUNEL assay indicated that complexes (0.34 μg/mL for **C1**, 0.30 μg/mL for **C2**, 0.29 μg/mL for **C3**, 0.38 μg/mL for **C4** and 0.13 μg/mL for **C5**) caused more intense apoptosis in the HT29 cell line than positive control, 5FU.

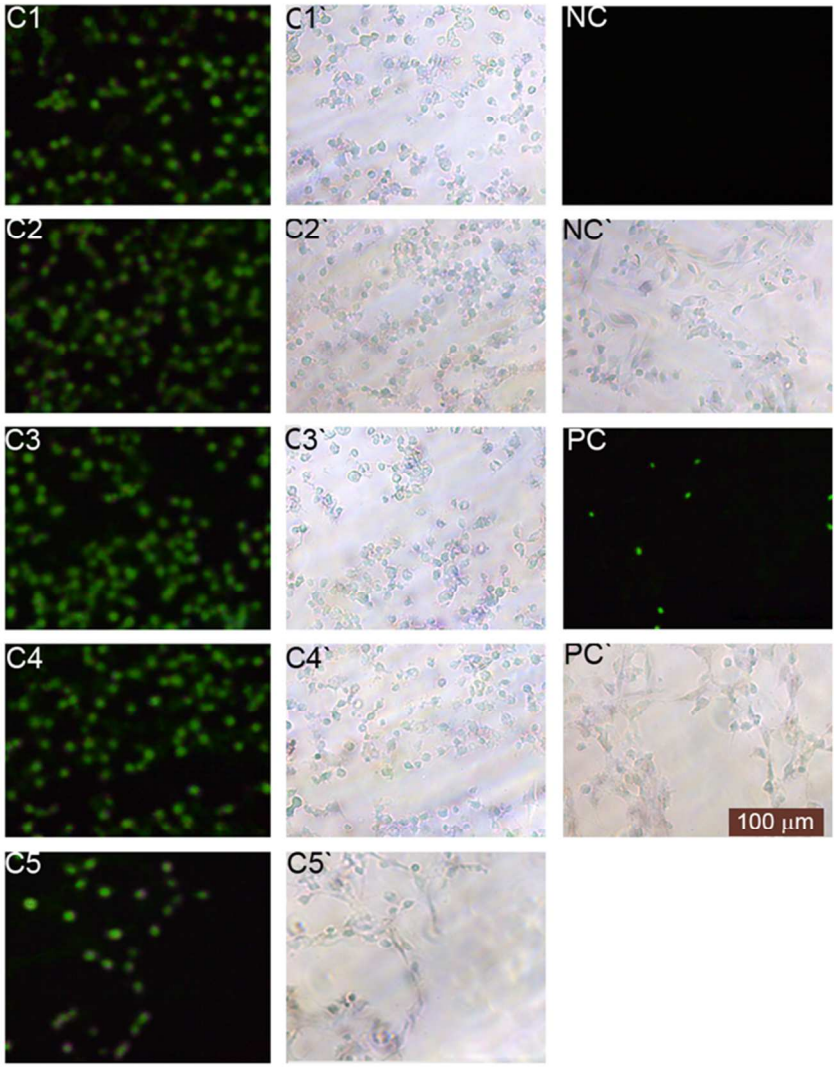

Fig 9. Fluorescence and phase-contrast images of the HT29 cancer cell line examined by TUNEL assay. TUNEL-positive cell nuclei with brilliant green were observed under a fluorescence (**C1**, **C2**, **C3**, **C4**, **C5**, **NC** and **PC**) and phase-contrast microscope (**C1`**, **C2`**, **C3`**, **C4`**, **C5`**, **NC`**, and **PC`**). **C1**, **C2**, **C3**, **C4** and **C5**: treatments, **NC**: negative control, **PC**: positive control).

V. Detection of migration inhibitory activity of **C1**, **C2**, **C3**, **C4** *and* **C5**

Metastasis of the cancer cells is very important characteristics and an excellent drug target for the metastatic cancer cells. The antimetastatic potential of test compounds on HeLa cell lines was investigated using migration assay. It is found that test compounds at IC50 concentrations showed suppressive effect on the migration of HeLa cell line in a time-dependent manner, Supplementary Figure S14. Therefore, it is suggested that test compounds may have antimetastatic potential.

VI. Detection of DNA topoisomerase I inhibitory activity of **C1**, **C2**, **C3**, **C4** *and* **C5**

DNA topoisomerase I is a nuclear enzyme that plays essential roles in controlling the topological state of DNA to facilitate and remove barriers for vital cellular functions, including DNA replication and repair. The DNA topoisomerase I inhibitory activities of test compounds were determined by DNA topoisomerase I inhibition assay. As shown in Figure 10, these compounds failure to inhibit the DNA relaxation activity of DNA topoisomerase I, indicating that their mechanism of action for inhibition of cell proliferation may not involve inhibition of DNA topoisomerase.

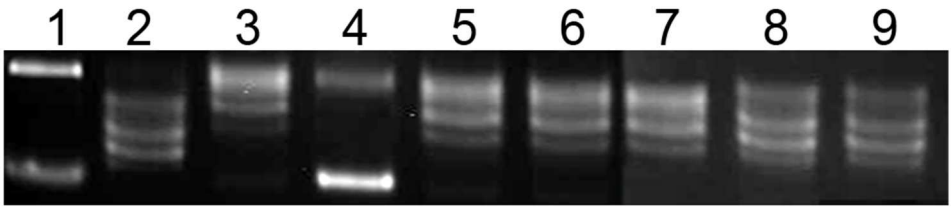

Fig 10. Inhibition of recombinant human topoisomerase I activity by test compounds. The super coiled plasmid DNA was incubated with DNA topoisomerase I only and DNA topoisomerase I plus **C1**, **C2**, **C3**, **C4**, **C5** and Camptothecin. The results showed that **C1**, **C2**, **C3**, **C4** and **C5** failure to inhibit DNA relaxing activity of DNA topoisomerase I. Lane 1: Supercoiled marker DNA; Lane 2: Relaxed marker DNA; Lane 3: Negative Control (Supercoiled DNA + Topo I); Lane 4: Positive Control (Supercoiled DNA + Topo I + Camptothecin); Lane 5: Supercoiled DNA + Topo I + **C1**; Lane 6: Supercoiled DNA + Topo I + **C2**; Lane 7: Supercoiled DNA + Topo I + **C3**; Lane 8: Supercoiled DNA + Topo I + **C4**; Lane 9: Supercoiled DNA + Topo I + **C5**.

VII. The effect of **C1**, **C2**, **C3**, **C4** *and* **C5** *on the morphology of HeLa, HT29 and C6 cells*

The effect of the test compounds on the morphology of HeLa, HT29 and *C6* cells were shown in Supplementary Figure S15. The compounds were clearly inhibited elongation and growth of the cells in culture. All cells were very weakly attached the surface of culture plate and become globular upon treatment. *C6* and HT29 cells were lost their fibroblast like appearance and HT29 cells clumped together.

Cancer is one of the most important health problems in the world. It proposed that it will affect in 20 million people by 2020.[53] Therefore more significant advancements are needed to cure cancer effectively. The use of metals in medicine dates back to antiquity, with various complexes being used to treat different ailments. Even today, metal complexes and their application in medicine have been studied extensively (REFs). The beginning in the modern sense of cancer chemotherapy has been accepted as the fortuitously discovery of the mechlorethamine (mustine) and cisplatin.[54] Thus, metal containing complexes are widely used in treatment of cancers such as leukopenia and prostate tumors. However, they have shown to have significant side effects and drug resistance during its clinical applications. Therefore, development of novel anticancer drug candidates with little or no side effects is still important.

It is known that some metal complexes such as *cis*platin binds biomolecules like DNA, RNA, protein and others. In recent years, various silver and gold complexes have been reported to have anti-cancer activity in vitro. For example, Vančo et al.[55] found that gold(I) mixed-ligand complexes involving *O*-substituted derivatives of 9-deazahypoxanthine (HLn) and triphenylphosphine (PPh_3) with the general formula [Au(Ln)(PPh_3)] possess anti-cancer and anti-inflammatory activity against certain types of cancer. Korkmaz et al[39] reported [Ni(*hydeten*)$_2$Ag(CN)$_2$][Ag(CN)$_2$]·H_2O, and [Cd_2(*hydeten*)$_2$ $Ag_4(CN)_8$]·H_2O where *hydeten* is N-(2-hydroxyethyl) ethylenediamine), and two novel cyanido-bridged bimetallic polymeric complexes possess anti-cancer activity against HeLa, HT29, *C6* and Vero cell lines. Liu et al.[56] showed that Au(I) and Ag(I) bidendate pyridyl phosphine complexes possess anticancer activity against cisplatin-resistant human cancer cells (CH1-cisR, 41M-cisR and SKOV-3) based on their lipophilicity. Furthermore, Au(III) compounds possess certain promising anti-cancer activities, as observed by Sun et al.[57] Many similar studies about Ag and Au complexes have been performed.[58]

In the present study, anticancer potential, cytotoxic activity, and apoptotic effect of **C1**, **C2**, **C3**, **C4** and **C5** were investigated on several tumor cell lines, such as Hela, HT29, and *C6*. According to the cell proliferation assay results, these compounds and $[Au(CN)_2]^-$ exhibited very high anti-proliferative activity than 5FU against several cancer cell lines (Fig. 6), indicating their anticancer potential, as in previous studies.[40,59-61] In LDH tests, these compounds showed the same cytotoxic effects as 5FU, whereas the $[Au(CN)_2]^-$ revealed higher cytotoxic effects than 5FU on cancer cell lines in a dose-dependent manner ($p<0.05$) (Fig. 7). Therefore, we suggest that these compounds may have cytostatic potential rather than cytotoxic potential. We compared antiproliferative and cytotoxic activities of complexes and $[Au(CN)_2]^-$ to reveal the contribution of $[Au(CN)_2]^-$ to the activities of test compounds. As shown Figure 6 and 7, the antiproliferative and cytotoxic activities of test compounds were significantly lower than that of $[Au(CN)_2]^-$, indicating that the extreme cytotoxicity of $[Au(CN)_2]^-$ decreased to levels of 5FU in **C1**, **C2**, **C3**, **C4**, and **C5**. Previous studies showed that the anti-proliferative and cytotoxic effects of many Au complexes are consistent with this study.[62,63] Since the mechanism of action of many anticancer drugs involve apoptosis, we have tested the apoptotic potential of the complexes on the HT29 cell line using TUNEL assay. As illustrated in Figure 9, the TUNEL results clearly show that the test compounds significantly induced apoptosis on HT29 cells indicating that **C1**, **C2**, **C3**, **C4** and **C5** inhibit cell proliferation by inducing apoptosis, as in previous studies by Marzano et al.and To et al..[62,63] DNA degradation tests, these complexes resulted in the DNA laddering activity of complexes on cells degradation tests, was further confirm the these complexes resulted in the DNA laddering of cancer cell DNA, indicating their apoptotic potential of the complexes (Figure 8). It is known that cisplatin-like metallo-drugs inhibit cell proliferation by binding to cell DNA; however, it is not clear yet whether test compounds bind to cell DNA. The Au(I) complexes caused a dose-dependent induction of apoptosis in cancer cells, primarily through a group of protease-mediated pathways, as suggested by the ability of DNA laddering in coordination-polymer-treated cells. Typical results from cancer cells treated with each compound are shown in Figure 8. These compounds induced the formation of DNA fragmentation in cancer cell lines compared to the control cells (Fig. 8). In untreated cells, there was no DNA fragmentation, and intact genomic DNA was situated near the well at the top of the lanes. These results were somewhat similar to those of previous studies by Hall et al., Rackham et al., Wang et al., Wang et al., and Palanichamy et al..[64-68] The primary target for test compounds may be DNA, RNA or cellular macro proteins and cellular death is caused by irreversible affects these complexes. However, the molecular mechanisms of action of test compounds are still largely unknown. DNA topoisomerases are very effective antitumor targets because of their

essential function of regulating DNA topology during DNA replication and recombination.[69] Several important topoisomerase inhibitors such as camptosar, irinotecan, and topotecan have been used in routine clinical practice. There has been continuous interest in studying and developing new anti-topoisomerase agentsc.[70-72] The effects of test compounds on topoisomerase I-mediated supercoiled pHOT1 relaxation were investigated. The results revealed that the IC_{50} concentration of test compounds failed to show any effect on topoisomerase I (Fig.10). Recent work showed that a gold(III) complexes of pyridyl- and isoquinolylamido ligands displayed significant anti-topoisomerase activity in cancer lines, whereas a study that gold(I) complexes with anti-topoisomerase activity was not found in the literature.[73] Test compounds may also cause modulated cell death and apoptotic stress resulting from cell migration, which are both processes that are intimately involved in cancer progression. Test compounds can restrict the levels of migration of HeLa cancer cells, so they should therefore be used in association with anti-cancer drugs to fight cancer (Supplementary Figure S14). Test compounds were found to inhibit tumor cell migration with low cytotoxicity. Most cancer cells are defined by a more robust invasive potential than normal cells. A successful cancer treatment is required to suppress cancer cell proliferation and migration potential, since cancer cells escaping from the primary tumor site colonize different metastatic sites. This study showed for the first time that test compounds are able to reduce HeLa cell migration and most likely decrease the expression of the surface-expressed ligands such as growth factors. With regard to morphology of cells was investigated using phase-contrast microscopy. As shown in Figure 12, obvious morphological changes were observed in the treated cells as a dose-dependent manner compared to the untreated cells. Each cell lines exposed to the compounds exhibited cytoplasmic blebs, shrinkage, anomalous globular structure and appearance of apoptotic bodies as apoptotic indicators (Supplementary Figure S15). This was consistent with the results of the BrdU cell proliferation ELISA assay and DNA laddering test. Thus, based on these observations in the literature, the appearance of the cell lines treated with test compounds were clearly indicated the anti-proliferative and low cytotoxic effect of these complexes. Moreover, the results of DNA fragmentation assays and TUNEL assay indicate that these novel complexes may inhibit cell proliferation through induction of apoptosis. These results were somewhat similar to previous studies by Casini et al.,[74] Zhang et al.,[75] and Cattaruzza et al.[76] To sum up, we have demonstrated for the first time that **C1**, **C2**, **C3**, **C4** and **C5** a strong apoptosis-inducer, possesses vigorous inhibitory effects on cancer cell lines *in vivo*. Based on our results, it is suggested that both complexes are potential and valuable anti-cancer drug candidates to be used in medicine as suitable candidates for further pharmacological testing. We believe that there is a great need for large and well-designed anti-cancer activity studies of new anti-cancer agents with better solubility in biological fluid and less toxicity built from parent compound test compounds**.** In conclusion, our results have demonstrated that metal complexes **C1**, **C2**, **C3**, **C4** and **C5** are potent anticancer drug candidates with higher antiproliferative, low cytotoxic, strong apoptosis-inducing and effective DNA topoisomerase inhibitory characteristics. However, further *in vitro* and *in vivo* studies need to be performed to verify their anticancer drug potential.

CONCLUSIONS

Five new cyanido-bridged polymeric complexes with $[Au(CN)_2]^-$ and *hydeten;* N-(2-hydroxyethyl)-ethylenediamine were synthesized, characterized, and tested their biological activities (antibacterial, antifungal and anticancer) as *in vitro*. The chemistry of *hydeten* ligand has been under study for the past decade, but this interaction with $[Au(CN)_2]^-$ is described here for the first time.

We have strongly demonstrated that five new cyanido-bridged coordination polymers have a great potential as an antitumor agents. The main reason for this is that coordination polymers have the major advantage stemming from the low application dose and physiologically stable. The results clearly describe not only a high antiproliferative effect but also a low cytotoxic affect, depending on the ligand coordinated to the metal ions. Worthy mentioning is the potent apoptotic activity developed by coordination polymers in the *in vitro* studies. The *in vitro* studies also showed that coordination polymers were found to behave as potential antimetastatic and antimigratory agents against HeLa cells. Treatment with the coordination compounds cannot inhibit topoisomerase I, which is required for cell proliferation. The free ligand show quite remarkable antiproliferative activity, but it increases the cytotoxicity around six times. To sum up, it was shown that the antiproliferative activity of these coordination polymers appears to be a function of the nature of the ligand, coordination polymers structure, the stability in physiological solution, and the incubation time. Based on our results, it is suggested that five new cyanido-bridged coordination polymers are potentially valuable antitumor drug candidates and are suitable for further pharmacological testing.

EXPERIMENTAL

Synthetic Procedure

$K[Au(CN)_2]$ (Aldrich), $Ni(ClO_4)_2.6H_2O$ (Alfa Aesar), $Cu(ClO_4)_2.6H_2O$ (Aldrich), $Zn(ClO_4)_2.6H_2O$ (Aldrich), $CdSO_4.8/3H_2O$ (Sigma-Aldrich) and N-(2-hydroxyethyl)-ethylenediamine (*hydeten*) (Aldrich) were used as received.

The preparation of the complexes was performed using general procedure the so-called "*brick* and *mortar*".[77] N-(2-hydroxyethyl)-ethylenediamine (1 mmol or 2 mmol) was added to aqueous solution of Ni, Cu, Zn and Cd salts (1 mmol). Then, the mortar solution prepared in water-ethanol (1:1) mixture, $K[Au(CN)_2]$ (1 mmol) was added to formed brick solution, $[M(hydeten)_n]^{2+}$, (n= 1 or 2) and the mixture was stirred for about 3 hours. The resulting solutions were left to stand at room temperature and allowed to evaporate slowly over a few days for crystallization. Finally, the powder crystals of **C1** and **C2** and the single crystals of **C3**, **C4** and **C5** were obtained from this solution.

Anal. Calc. (%) for $C_8H_{12}N_6OAu_2Ni$ (**C1**): *C* 14.54, *H* 1.83, *N* 12.72, found: *C* 15.13, *H* 2.13, N 12.47. IR spectra (KBr disk cm^{-1}) 3303, 3239 [υ(N–H)]; 3363 [υ(O–H)]; 2977, 2950, 2886 [υ(C–H)]; 2173 [υ(C≡N)]; 1589 [δ(N–H)]; 1047 [υ(C-O)].

Anal. Calc. (%) for $C_{12}H_{26}N_8O_3Au_2Ni$ (**C2**): *C* 18.41, *H* 3.35, *N* 14.31, found: *C* 18.79, *H* 3.55, *N* 14.01. IR spectra (KBr disk cm^{-1}) 3291, 3268 [υ(N–H)]; 3357 [υ(O–H)]; 2948, 2877 [υ(C–H)]; 2169,2146 [υ(C≡N)]; 1602 [δ(N–H)]; 1054 [υ(C-O)].

Anal. Calc. (%) for $C_{13}H_{28}N_8O_3Au_2Cu$ (**C3**): *C* 19.47, *H* 3.52, *N* 13.97, found: *C* 19.71, *H* 3.51, *N* 13.73. IR spectra (KBr disk cm^{-1}) 3334, 3301, 3257, 3160 [υ(N–H)]; 3569, 3478, 3411 [υ(O–H)]; 2944, 2881 [υ(C–H)]; 2144 [υ(C≡N)]; 1596 [δ(N–H)]; 1064 [υ(C-O)].

Anal. Calc. (%) for $C_{12}H_{26}N_8O_3Au_2Zn$ (**C4**): *C* 18.25, *H* 3.32, *N* 14.19, found: *C* 18.48, *H* 3.41, *N* 13.91. IR spectra (KBr disk cm^{-1}) 3291, 3266 [υ(N–H)]; 3361 [υ(O–H)]; 2946, 2877 [υ(C–H)]; 2167, 2144 [υ(C≡N)]; 1600 [δ(N–H)]; 1054 [υ(C-O)].

Anal. Calc. (%) for $C_{12}H_{24}N_8O_3Au_2Cd$ (**C5**): *C* 17.27, *H* 2.90, *N* 13.47, found: *C* 18.11, *H* 3.18, *N* 13.68. IR spectra (KBr disk cm^{-1}) 3295, 3266 [υ(N–H)]; 3361 [υ(O–H)]; 2948, 2877 [υ(C–H)]; 2163, 2142 [υ(C≡N)]; 1600 [δ(N–H)]; 1054 [υ(C-O)].

Physical Measurements

Elemental analyses (C, H and N) were performed using a LECO CHNS-932 elemental analyzer. IR spectra were measured on a Jasco 430 FT-IR spectrometer using KBr pellets in the 4000–400 cm^{-1} range. Thermogravimetric analyses were carried out on Perkin-Elmer Diamond TG/DTA Thermal Analysis instrument in a nitrogen atmosphere with a heating rate of 10 ºCmin^{-1} and a 10 mg sample.

Crystallography

For the crystal structure determination, the single-crystals of $[Cu(hydeten)_2Au_2(CN)_4].CH_3OH$ (**C3**), $[Zn(hydeten)_2Au_2(CN)_4].H_2O$ (**C4**) and $[Cd(hydeten)_2Au_2(CN)_4].H_2O$ (**C5**) were used for data collection on a Stoe-IPDS imaging plate diffractometer with monochromatized MoK_α radiation (λ=0.71073 Å). Data collection: X-Area, cell refinement: X-Area, data reduction: XRED.[78] The structure was solved by direct methods and was refined using the programs SHELXS-97 and SHELXL-97.[79] All of the non-hydrogen atoms were refined anisotropically, and the hydrogen atoms attached to carbon were located at their ideal positions. The packing and ORTEP-type diagrams were obtained by using DIAMOND 3.0 (Demonstrated Version).[80] Further details are given in Table 9.

As showed by detailed research, the crystal structure of **C3** exhibits positional disorder in distribution of *hydeten* and hydroxyethyl group. Thus, the atoms of these groups are both split in two positions with 0.45(2):0.55(2) occupancy ratio. The solvent methanol also shows a symmetry related disorder. The water H-atoms could not be reliably located because of the water molecule O1W lies onto a glide plane and therefore they were not included in the final molecular model for **C5**.

Table 9 Crystal data and structure refinement for **C3**, **C4** and **C5**

Identification code	**C3**	**C4**	**C5**
Empirical formula	$C_{13}H_{28}N_8O_3CuAu_2$	$C_{12}H_{26}N_8O_3ZnAu_2$	$C_{12}H_{24}N_8O_3CdAu_2$
Formula weight	801.91	789.71	836.74
Temperature/K	293(2)	293(2)	293(2)
Crystal system	Monoclinic	Monoclinic	Monoclinic
Space group	I2/a	I2/a	I2/a
a/Å	11.6556(9)	10.8950(6)	11.0302(9)
b/Å	14.2528(15)	12.6494(6)	13.1045(6)
c/Å	13.4694(12)	15.5745(9)	15.5492(11)
α/°	90.00	90.00	90.00
β/°	98.262(7)	101.857(5)	101.280(6)
γ/°	90.00	90.00	90.00
Volume/$Å^3$	2214.4(3)	2100.6(2)	2204.1(3)
Z	4	4	4
$\rho_{calc}g/cm^3$	2.405	2.497	2.522
μ/mm^{-1}	14.198	15.094	14.262
F(000)	1492.0	1464.0	1536.0
Radiation	MoKα (λ = 0.71073)	MoKα (λ = 0.71073)	MoKα (λ = 0.71073)
2Θ range for data collection/°	4.18 to 50.98	4.18 to 56.42	4.1 to 52
Index ranges	$-14 \le h \le 14$, $-17 \le k \le 15$, $-16 \le l \le 16$	$-14 \le h \le 11$, $-16 \le k \le 16$, $-20 \le l \le 20$	$-10 \le h \le 13$, $-16 \le k \le 14$, $-19 \le l \le 19$
Reflections collected	6138	7555	5669

Independent reflections	2069 [R_{int} = 0.1357, R_{sigma} = 0.0879]	2596 [R_{int} = 0.0591, R_{sigma} = 0.0539]	2158 [R_{int} = 0.0980, R_{sigma} = 0.0636]
Data/restraints/parameters	2069/209/181	2596/2/127	2158/0/121
Goodness-of-fit on F^2	1.089	0.947	1.069
Final R indexes [I>=2σ (I)]	R_1 = 0.0588, wR_2 = 0.1617	R_1 = 0.0363, wR_2 = 0.0820	R_1 = 0.0428, wR_2 = 0.1031
Final R indexes [all data]	R_1 = 0.0572, wR_2 = 0.1350	R_1 = 0.0536, wR_2 = 0.0869	R_1 = 0.0509, wR_2 = 0.1070
Largest diff. peak/hole / e $Å^{-3}$	1.82/-1.34	1.39/-1.49	1.32/-2.01
CCDC deposition number	1040941	1040942	1040943

Biological Studies

Test microorganisms

The antibacterial activity of chemicals was assessed against four gram (+); *Staphylococcus aureus* ATCC 25213, *Enterococcus faecali s*ATCC51299., *Bacillus cereus* DSM4312, *Bacillus subtilis*ATCC6633, five gram (-) bacteria species:*Escherichia coli* ATCC 11229, *Pseudomonas aeruginosa* ATCC29213, *Salmonella enteritidis*ATCC13076, *Proteus vulgaris*Kuen1329, *Klebsiella pneumonia* ATCC700603 and one yeast: *Candida albicans* ATCC1223. The strains were maintained on Brain Heart Infusion (BHI) agar medium or Potato Dextrose Agar (PDA) at 4 ºC until testing. Activated overnight cultures were incubated for 18 h at 36ºC ± 1ºC and then bacterial suspension was diluted with sterile physiological solution to 10^8CFU/mL (turbidity = McFarland barium sulfate standard 0.5) for the agar spot tests.[81]

Spot on lawn method

Antibacterial tests were carried out by the spot on lawn method using 100 mL of suspension containing 10^8 CFU per mL of bacteria and 10^6 CFU per mL of yeast spread on Mueller Hinton Agar (MHA) medium.[82] 5 µL of chemical suspensions (5µg per spot) were spotted on air-dried MHA plates. The inoculated plates were incubated at 36 ºC for 24 h. Ampicillin (100 µg) was used as positive control and KCN suspension or DMSO was used as negative control. Antibacterial activity was evaluated by measuring the zone of inhibition in mm against the test organisms. Each test was run in triplicate.

Determination of Minimum Inhibitory Concentrations (MIC)

Agar spot method of Wiegand et al.[83] with modifications was used to determinethe MIC of the chemicals. Briefly 100 µL of bacteria cultures were spread onto Mueller Hinton Agar (MHA) plates. Then, serial dilutions of chemicals were made in a concentration range from 15.62–2000 µg/mL inappropriate solutions (Water or dimethylsulfoxide (DMSO)).5 µL of chemical suspensions were spotted on air-dried MHA plates.The inoculated plates were incubated at 36 ºC for 24 h. Ampicillin (100 µg) was used as positive control and KCN suspension or DMSO was used as negative control. The lowest concentration at which there was no visible zone of inhibition was taken as the MIC. And the inhibitionzone produced by each compound was measured in mm.Each test was run in triplicate.

Antifungal activity assay

Antifungal activity assay was carried out by agar well diffusion method.[84] The following soil born imperfect fungi were used: *Alternari solani*, *Fusarium oxysporum*, and *Rhizoctonia solani* fungal isolates were from culture collection at Department of Plant Protection,

Agricultural Faculty, Gaziosmanpasa University, Tokat. Appropriate wells (5 mm diameter) were made on PDA plate by using cork borer and five different doses of the **C1**, **C2**, **C3**, **C4**, **C5** (5, 7.5, 10, 15 ve 20 µg/mL), negative control (20 µg/mL of 50% DMSO) and fungicides (Copper hydroxide (1.25 mg/mL) and Maneb (2.4 mg/mL)) were loaded. Mycelial disc (5 mm in diameter) of the fungus was cut from the periphery of the active growth culture (72 hours old) and was placed upside down on the PDA plates 30 mm a part from well compound was loaded. Plates were sealed with parafilm incubated for 5 days at room temperature (25 ±2 ^{0}C). The antifungal activity was observed for appearance of zones of inhibition after 72hrs incubation period.[85] The experiment was carried out in 3 replicates.

Statistical analysis

Analysis of variance (ANOVA) was used to determine the effects of the compounds **C1**, **C2**, **C3**, **C4** and **C5** on mycelial growth of fungi. Statistical analysis was performed with SAS (version 9.1.3) statistic software. Inhibition zone data was analyzed using POLO-PC Probit[86] to estimate lethal concentration 50 value (LC50) and the regression line slope.

Cell culture

C6, HT29, HeLa, and Vero cell lines[87-89] were maintained in Dulbecco's modified Eagle's medium (DMEM, Sigma, Germany) supplemented with 10% (v/v) fetal bovine serum (Sigma) and PenStrep solution (10,000 U/10 mg) (Sigma). At confluence, cells were detached from the flasks using 4 mL of trypsin-EDTA (Sigma) and centrifuged, and the cell pellet was resuspended with 4 mL of supplemented DMEM.

Cell proliferation assay

A cell suspension containing 3×10^3 cells in 100 µL was pipetted into the wells of 96-well cell culture plates (COSTAR, Corning, USA). The test compounds (**C1**, **C2**, **C3**, **C4**, **C5** and $[Au(CN)_2]^-$) and a positive control compound (5FU) were dissolved in sterile dimethyl sulfoxide (DMSO). The amount of DMSO was adjusted to 0.5% maximum. The cells were treated with test compounds, $[Au(CN)_2]^-$, and 5FU at final concentrations of 0.05, 0.10, 0.20, 0.30, 0.40, 0.50, 0.75, and 1.00 µg/mL. Cell controls and solvent controls were treated with supplemented DMEM and sterile DMSO, respectively. The final volume of the wells was adjusted to 200 µL by supplemented DMEM. The cells were then incubated at 37°C with 5% CO_2 overnight. The antiproliferative activity of the compounds was determined using a BrdU cell proliferation enzyme-linked immunosorbent assay (ELISA) kit according to the manufacturer's protocol (Roche, USA) for a calorimetric immunoassay based on BrdU incorporation into the cellular DNA. Briefly, cells were exposed to BrdU labeling reagent for 4 h, followed by fixation in FixDenat solution for 30 min at room temperature. Cells were then cultured with a 1:100 dilution of anti-BrdU-POD for 90 min at room temperature. Substrate solution was added to each well, and BrdU incorporation was measured at 450–650 nm using a microplate reader (Rayto, China). Each experiment was repeated at least 3 times for each cell line.

Calculation of IC_{50} and % inhibition

IC_{50} represents the concentration of an agent that is required for 50% inhibition in vitro. The half maximal inhibitory concentration (IC_{50}) of the test and control compounds was calculated using XLfit5 software (IDBS) and expressed in µg/mL at 95% confidence intervals. The cell

proliferation assay results were reported as the percent inhibition of the test and control substances. The percent inhibition was calculated according to the following formula: % inhibition = [1 -(absorbance of treatments / absorbance of DMSO) × 100].

Cytotoxic activity assay

The cytotoxicity of test compounds, $[Au(CN)_2]^-$, and 5FU on *C6*, HT29, HeLa, and Vero cells was determined with a LDH cytotoxicity detection kit (Roche) based on the measurement of LDH activity released from the cytosol of damaged cells into the supernatant according to manufacturer's instructions. Briefly, $3x10^4$ cells in 100 µL were seeded into 96-well microtiter plates as triplicates and treated with IC_{50} concentrations of **C1**, **C2**, **C3**, **C4**, **C5** and $[Au(CN)_2]^-$ as described above at 37°C with 5% CO_2 overnight. LDH activity was determined by measuring absorbance at 492–630 nm using a microplate reader.

Analysis of DNA laddering

DNA laddering effect of the test compounds was measured according to the method of Gong[90] with some modifications. Briefly, $7.5x10^5$ cells were seeded into 25 cm^2 culture flasks, and treated with IC_{50} concentrations of test compounds at 37°C with 5% CO_2 for overnight. Treated cells were harvested using a sterile plastic scraper, transferred to a 15 mL sterile Falcon tube, washed with 1 mL sterile DPBS, and pelleted by spinning at 1500xg for 5 min. The cell pellet resuspended with 200 µL ice cold DPBS by gently pipeting, fixed with 5 mL ice cold 70% ethanol, vortexed shortly and incubated at -20°C for 24 hours. The cells were centrifuged at 1500xg for 5 min, the supernatant was removed and the remaining ethanol removed by air drying. The cell pellet was resuspended in 50 µL phosphate-citrate buffer (consisting of 192 parts of 0.2 M Na_2HPO_4 and 8 parts of 0.1 M citric acid, pH 7.8), incubated at 37°C for 30 min in a shaker incubator, and centrifuged at 1500xg for 5 min. A 40 µL of supernatant was transferred to a 1.5 mL microsantrifuge tube, mixed with 5 µL Tween20 solution (%0.25 in ddH_2O) and 5 µL RNase A solution and incubated at 37°C for 30 min in a shaker incubator. Then, 5 µL proteinase K was added to each tube and incubated at 37°C for 10 min. Finally, the entire content of the microcentrifuge tube was mixed with 4 µL of 6x loading buffer, loaded to 1.5% agarose gel containing 0.5 µg/mL ethidium bromide and electrophoresed at 200 mA for 40 min. DNA laddering in the gels was visualized using gel documentation system (UVP, England).

TUNEL assay

In vitro detection of apoptosis was assessed using a TUNEL assay kit (Roche) according to the manufacturer's protocol. HT29 cell lines (30,000 cells/well) were placed in a poly-L-lysine covered chamber slide. The cells were treated with the IC_{50} concentrations of test compounds and left for 24 h of incubation. There were 2 controls for this assay: a positive control that had DNase I treatment, and a negative control that had no terminal deoxynucleotidyl transferase (TdT). When the incubation time was over, the chamber was removed from the slide and washed with Dulbecco's phosphate buffered saline (DPBS) to remove the medium and unattached cells. All of the incubation and washing steps were done in a plastic jar. Slides were gently washed with DPBS, and, for fixation, 4% paraformaldehyde in DPBS at pH 7.4 was freshly prepared and added to the slides for 60 min at room temperature. Following incubation, the slides were washed twice with DPBS. The cells were blocked with freshly prepared 3% H_2O_2 in methanol for 10 min at room temperature. Following incubation, the slides were washed twice with DPBS. The cells were permeabilized by prechilled 0.1% Triton X-100 and freshly prepared 0.1% sodium citrate in water and then incubated for 2 min on ice. All the slides were washed with DPBS twice for 5 min each. At this point, in order to prepare a DNase I enzyme-

treated positive control, 100 μL of DNase I buffer was added to the slide and incubated at room temperature for 10 min. Fixative cells were transferred into a TUNEL reaction mixture (50 μL/section) containing TdT and fluoresceindUTP. Intracellular DNA fragments were then labeled by exposing the cells to the TUNEL reaction mixture for 1 h at 37°C in a humidified atmosphere, protected from light. After washing with DPBS twice, cells positive for apoptosis showed a green fluorescent signal and were visualized by a Leica fluorescent microscope (Leica DMIL LED Fluo, Germany).

Cell migration assay

The migration inhibitory capability of the compounds was measured using the cell migration assay. Briefly, a culture insert (ibidi GmbH, Germany) consists of two reservoirs separated by a 500 μm thick wall, was placed on a 35-mm petridish, and an equal number of HeLa cells (3.5×10^4 HeLa cells in 70 μL DMEM medium) were seeded into the two reservoirs of the same insert and allowed to grow to 90–95% confluence, in order to generate a 500 μm gap between two cell populations. Subsequent to cell growth, the insert was gently removed and 2 ml of cell culture medium was added and treated with IC_{50} concentrations of test compounds for overnight at 37°C with 5% CO_2. The closure of the gap by the cells was photographed 0, 1 and 2 days after incubation by using a phase contrast inverted microscope (Leica DMIL, Germany).

DNA topoisomerase I inhibition assay

The DNA topoisomerase I inhibitory activities of **C1**, **C2**, **C3**, **C4** and **C5** were evaluated using a cell-free topoisomerase I assay kit (TopoGen, USA). The principle of the assay is to measure the conversion of supercoiled pHOT1 plasmid DNA to its relaxed form in the presence of DNA topoisomerase I alone and with test compounds. The supercoiled substrate (pHOT1 plasmid DNA) and its relaxed product can easily be distinguished in agarose gel, because the relaxed isomers migrate more slowly than the supercoiled isomer. In brief, 20 μL of reaction mixture containing 1 μL of plasmid pHOT1 DNA in relaxation buffer was incubated with 2 U of recombinant human topoisomerase I enzyme in the presence of IC_{50} concentrations of test compounds, or camptothecin as a positive control. The reactions were carried out at 37 °C for 30 min and then terminated by the addition of stop solution. After the termination, the sample was analyzed using 1% agarose gel at 4 V/cm for 60 min. After electrophoresis, DNA bands were stained with ethidium bromide (1 mg/mL) solution and photographed with a gel imaging system (UVP BioSpectrum, Germany).

Cell imaging

Cells were seeded in 96-well plates at a density of 5,000 cells per well and allowed 24 h for attachment. Using previously established IC_{50} doses of test compounds treatment was performed for 24 h, during which morphology changes were assessed by phase contrast microscopy. Images of vehicle (DMSO), **C1**, **C2**, **C3**, **C4** and **C5** treated cells were taken at the end of experimental period using a digital camera attached inverted microscope (Leica IL10, Germany).

Statistical analysis

The statistical significance of differences was determined by one-way analysis of variance (ANOVA) tests. Post hoc analyses of group differences were performed using the Turkey test, and the levels of probability were noted. SPSS for Windows was used for statistical

analyses. The results are reported as the mean values ± standard error of the mean (SEM) of 3 independent assays, and differences between groups were considered to be significant at $P<0.05$.

ACKNOWLEDGMENT

We gratefully acknowledge the Scientific and Technical Research Council of Turkey (TUBITAK, Grant TBAG-112T696; COST Action CM 2515).

NOTES and REFERENCES

[a]Gaziosmanpaşa University, College of Art and Science, Department of Chemistry, 60240, Tokat, TURKEY; Tel: +90 356 252 1616 / 3066, 3058; ahmet.karadag@gop.edu.tr, sureyyadede@gmail.com

[b]Department of Molecular Biology and Genetics, Gaziosmanpaşa University, 60240, Tokat, TURKEY; aliaydin.bio@gmail.com saban.tekin@gop.edu.tr

[c]Department of Plant Protection, Faculty of Agriculture, Gaziosmanpaşa University, 60240, Tokat, TURKEY; yusuf.yanar@gop.edu.tr

[d]Department of Bioengineering, Engineering and Natural Science Faculty, Gaziosmanpaşa University, 60240, Tokat, TURKEY; bilgehilal.cadirci@gop.edu.tr

[e]Giresun University, Faculty of art and sciences, Department of Physics, 28100, Giresun, TURKEY; mustafa.serkan.soylu@giresun.edu.tr

[f]Ondokuzmayıs University, College of Art and Science, Department of Chemistry, 55139, Samsun, TURKEY; Tel: +90 362 312 1919 / 5455; oandac@gmail.com

Cambridge Crystallographic Data Centre [CCDC ID: 1040941 (**C3**), 1040942 (**C4**) and 1040943 (**C5**)]. Copies of the data can be obtained free of charge at www.ccdc.cam.ac.uk. or from the Cambridge Crystallographic Data Centre, 12 Union Road, Cambridge CB2 1EZ, UK (fax: +44-1223-336033 or e-mail: deposit@ccdc.cam.ac.uk)].

REFERENCES

1. M. Tadokoro, S. Yasuzuka, M. Nakamura, T. Shinoda, T. Tatenuma, M. Mitsumi, Y. Ozawa, K. Toriumi, H. Yoshino, D. Shiomi, K. Sato, T. Takui, T. Mori and K. Murata, *Angew. Chem. Int. Ed*., 2006 **45**(31) 5144-5147.

2. D. L. Turner, T. P. Vaid, P. W. Stephens, K. H. Stone, A. G. DiPasquale and A. L. Rheingold, *J. Am. Chem. Soc*., 2008, **130**(1), 14-15.

3. M. Ohba and H. Okawa, *Coord. Chem. Rev.*, 2000, **198**, 313-328.

4. W. Kaneko, S. Kitagawa and M. J. Ohba, *J. Am. Chem. Soc*., 2007, **129**, 248-249.

5. S. R. Batten and K. S. Murray, *Coord. Chem. Rev*., 2003, **246**, 103-130.

6. C. Paraschiv, M. Andruh, S. Ferlay, M. W. Hosseini, N. Kyritsakas, J.-M. Planeix and N. Stanica, *Dalton Trans*., 2005, 1195-1202.

7. A. Karadağ, A. Şenocak, Y. Yerli, E. Şahin and R. Topkaya, *J Inorg Organomet Polym*., 2012, **22**, 369-378.

8. A. Şenocak, A. Karadağ, Y. Yerli, N. Gürbüz, İ. Özdemir and E. Şahin, *Polyhedron*, 2013, **49**, 50-60.

9. Ş. A. Korkmaz, A. Karadağ, N. Korkmaz, Ö. Andaç, N. Gürbüz, İ. Özdemir and R. Topkaya, J. Coord. Chem., 2013, **66**, 3072-3091.

10. Ş. A. Korkmaz, A. Karadağ, Y. Yerli, M. S. Soylu, *New J. Chem*., 2014, **38**, 5402-5410.

11. D. M. Rudkevich, *Angew. Chem. Int. Ed*., 2004, **43**(5), 558-571.

12. S. Kitagawa and K. Uemura, *Chem. Soc. Rev*., 2005, **34**, 109-119.

13. R. Banerjee, A. Phan, B. Wang, C. Knobler, H. Furukawa, M. O'Keeffe and O. M. Yaghi, *Science*, 2008, **319**, 939-943.

14. D. B. Leznoff, B.-Y. Xue, B. O. Patrick, V. Scanchez and R. C. Thompson, *Chem. Commun*., 2001, 259-260.

15. E. Colacio, F. Loret, R. Kivekäs, J. Ruiz, J. Suárez-Varela and M. R. Sundberg, Chem. Commun., 2002, **6**, 592-593.

16. D. B. Leznoff, B.-X. Xue, R. J. Batchelor, F. W. B. Einstein and B. O. Patrick, *Inorg. Chem*., 2001, **40**, 6026-6034.

17. E. Colacio, F. Lloret, R. Kivekäs, J. Ruiz, J. Suárez-Varela, M. R. Sundberg and R. Uggla, *Inorg. Chem.*, 2003, **42**(2), 560-565.

18. W. Dong, L.-N. Zhu, Y.-Q. Sun, M. Liang, Z.-Q. Liu, D.-Z. Liao, Z.-H. Jiang, S.-P. Yana and P. Chenga, *Chem. Commun*., 2003, 2544-2545.

19. H. H. Patterson, M. A. Rawashdeh-Omary, M. A. Omary and J. P. Fackler, *J. Am. Chem. Soc*., 2001, **123**, 11237-11247.

20. M. Stender, R. L. White-Morris, M. M. Olmstead and A. L. Balch, *Inorg. Chem.*, 2003, **42**, 4504-4506.

21. D. Z. Liao, W. Dong, L. N. Zhu, Y. Q. Sun, M. Liang, Z. Q. Liu, Z. H. Jiang, S. P. Yan and P, Cheng, *Chem. Commun*., 2003, **20**, 2544-2545.

22. A. Deák, T. Tunyogi, C. Jobbágy, Z. Károly, P. Baranyai and G. Pálinkás, *Gold Bull.*, 2012, **45**, 35-41.

23. M. J. Katz, T. Ramnial, H.-Z. Yu and D. B. Leznoff, *J. Am. Chem. Soc.*, 2008, **130**, 10662-10673.

24. D. B. Leznoff, J. Lefebvre and R. J. Batchelor, *J. Am. Chem. Soc*., 2004, 126, 16117-16125.

25. J. A. Real, A. Galet, M. C. Munoz and V. Martinez, *Chem. Commun*., 2004, **20**, 2268-2269.

26. J. A. Real, G. Agusti, A. B. Gaspar and M. C. Munoz, *Inorg. Chem*., 2007, **46**, 9646-9654.

27. J.´ Sua´rez-Varela, A. J. Mota, H. Aouryaghal, J. Cano, A. Rodrı´guez-Die´guez, D. Luneau, and E. Colacio, *Inorg. Chem*., 2008, **47**, 8143-8158.

28. E. T. Eisenmann, *J. Electrochem. Soc*., 1977, **124**(6), 819-826.

29. R. Eisler, *Inflamm Res*., 2003, **52**, 487-501.

30. G. G. Graham, M. W. Whitehouse and G. R. Bushell, *Inflammopharmacology*, 2008, **16**(3), 126-132.

31. A. Karadağ, H. Paşaoğlu, G. Kaştaş and O. Büyükgüngör, *Acta Crystallogr., Sect. C: Cryst. Struct. Commun.*, 2004, **60**, m581-m583.

32. A. Karadağ, A. Bulut and O. Büyükgüngör, *Acta Crystallogr., Sect. C: Cryst. Struct. Commun*., 2004, **60**, m402-m404.

33. A. Karadağ, H. Paşaoğlu, G. Kaştaş and O. Büyükgüngör, *Z. Kristallogr*., 2005, **220**, 74-78.

34. A. Karadağ, *Z. Kristallogr*., 2007, **222**, 39-45.

35. A. Karadağ, İ. Önal, A. Şenocak, İ. Uçar, A. Bulut and O. Büyükgüngör, *Polyhedron*, 2008, **27**, 223-231.

36. A. Karadağ, A. Şenocak, İ. Önal, Y. Yerli, E. Şahin and A. C. Başaran, *Inorganica Chimica Acta*, 2009, **362**, 2299-2304.

37. A. Karadağ, A. Bulut, A. Şenocak, İ. Uçar and O. Büyükgüngör, *J. Coord. Chem.*, 2007, **60**, 2035-2044.

38. H. Paşaoğlu, A. Karadağ, F. Tezcan and O. Büyükgüngör, *Acta Crystallogr., Sect. C: Cryst. Struct. Commun*., 2005, **61**, m93-m94.

39. N. Korkmaz, A. Karadağ, A. Aydın, Y. Yanar, İ. Karaman and Ş. Tekin, *New J. Chem*., 2014, **38**, 4760-4773.

40. A. Aydın, N. Korkmaz, Ş. Tekin and A. Karadağ, *Turk J Biol*., 2014, **38**, 948-955.

41. E. R. T. Tiekink, *Coord. Chem. Rev*., 2014, **275**, 130-153.

42. P. Pyykkö, *Angew. Chem. Int. Ed*., 43 (2004) 4412-4456.

43. H. Schmidbaur and A. Schier, *Chem. Soc. Rev*., 2008, **37**, 1931-1951.

44. S. Sculfort and P. Braunstein, *Chem. Soc. Rev*., 2011, **40**, 2741-2760.

45. P. Pyykkö, in: M.A. Johnson, T.J. Martinez (Eds.), *Ann. Rev. Phys. Chem*., 2012, **63**, 45-50.

46. X. He and V.W.-W. Vivian, *Coord. Chem. Rev*., 2011, **255**, 2111-2123.

47. H. Nie, M. J. Li, Y. J. Hao, X. D. Wang and X. S.-A. Zhang, *Chem. Sci*., 2013, **4**(4), 1852-1857.

48. M. J. Katz, K. Sakai and D. B. Leznoff, Chem. Soc. Rev., 2008, 37, 1884-1895.

49. H. E. Abdou, A. A. Mohamed, J. P. Fackler, A. Burini, R. Galassi, J. M. Lopez-de-Luzuriaga and M. E. Olmos, *Coord. Chem. Rev*., 2009, **253**, 1661-1669.

50. H. Schmidbaur and A. Schier, *Chem. Soc. Rev*., 2012, **41**, 370-412.

51. Z. D. Matović, V. D. Miletic, M. Cendic, A. Meetsma, P. J. Van Koningsbruggen and R. J. Deeth, *Inorg. Chem*., 2013, **52**(3), 1238-1247.

52. A. L. Spek, J. Appl. Crystallogr., 2003, **36**, 7-13.

53. M. Tuncer, *Cancer control in Turkey*, Ankara: Onur Press, Health Ministry Publication, 2008, **74**, 5-9.

54. D. E. Thurston, *Chemistry and Pharmacology of Anticancer Drugs*, Boca Raton, Florida, USA, CRC Press, 2007, 95-150.

55. J. Vančo, J. Gáliková, J. Hošek, Z. Dvořák, L. Paráková and Z. Trávníček, *Plos one*, 2014, **9**, 1-9.

56. J. J. Liu, P. Galettis, A. Farr, L. Maharaj, H. Samarasinha, A. C. McGechan, B. C. Baguley, R. J. Bowen, S. J. Berners-Price, and M. J. McKeage, *J. Inorg. Biochem*., 2008, **102**, 303-310.

57. R. W. Y. Sun and C. M. Che, *Coord. Chem. Rev*., 2009, **253**, 1682-1691.

58. V. Milacic, D. Fregona, and Q. P. Dou, *Histol Histopathol*, 2008, **23**, 101-108.

59. I. Ott, *Coord. Chem. Rev*., 2009, **253**, 1670-1681.

60. F. H. Kriel and J. Coates, *S. Afr. J. Chem*., 2012, **65**, 271-279.

61. F. Caruso, R. Villa, M. Rossi, C. Pettinari, F. Paduano, M. Pennati, M. G. Daidone, and N. Zaffaroni, *Biochem. Pharmacol*., 2007, **73**, 773-781.

62. C. Marzano, L. Ronconi, F. Chiara, M.C. Giron, I. Faustinelli, P. Cristofori, A. Trevisan and D. Fregona, *Int. J. Cancer*, 2011, **129**(2), 487-496.

63. Y. F. To, R. W. Y. Sun, Y. Chen, V. S. F. Chan, W.Y. Yu, P. K. H. Tam, C. M. Che and C. L. S. Lin, *Int. J. Cancer*, 2009, **124**, 1971-1979.

64. I.H. Hall, M. C. Miller and D. X. West, Met. *Based. Drugs*., 1997, **4**(2), 89-95.

65. O. Rackham, S. J. Nichols, P. J. Leedman, S. J. Berners-Price and A. Filipovska, *Biochem. Pharmacol*., 2007, **74**(7), (992-1002.

66. C. H. Wang, W. C. Shih, H. C. Chang, Y. Y. Kuo, W. C. Hung, T. G. Ong and W. S. Li, *J. Med. Chem*., 2011, **54**, 5245-5249.

67. Y. Wang, Q. Y. He, R. W. Sun, C. M. Che and J. F. Chiu, Eur. *J. Pharmacol*. 2007, **554**(2-3), 113-122.

68. K. Palanichamy, N. Sreejayan and A. C. Ontko, *J. Inorg. Biochem*., 2012, **106**(1), 32-42.

69. H. L. Zhu, X. M. Zhang, X.Y. Liu, X. J. Wang, G. F. Liu, A. Usman and H.K. Fun, *Inorg. Chem. Commun*., 2003, **6**, 1113-1116.

70. J. J. Champoux, *Annu. Rev. Biochem*., 2001, **70**, 369-413.

71. R. Prabhakaran, R. Sivasamy, J. Angayarkanni, R. Huang, P. Kalaivani, R. Karvembu, F. Dallemer and K. Natarajan, *Inorg. Chim. Acta*. 2011, **374**, 647-653.

72. X. Wu, J. C. Yalowich, B. B. Hasinoff, *J. Inorg. Biochem*. 2011, **105**(6), 833-838.

73. C. R. Wilson, A. M. Fagenson, W. Ruangpradit, M. T. Muller and O. Q. Munro, *Inorg. Chem*., 2013, **52**, 7889-7906.

74. A. Casini, M.A. Cinellu, G. Minghetti, C. Gabbiani, M. Coronnello, E. Mini and L. Messori, *J. Med. Chem*. 2006, **49**, 5524-5531.

75. C. X. Zhang and S. J. Lippard, *Curr. Opin. Chem. Biol*., 2003, **7**(4), 481-489.

76. L. Cattaruzza, D. Fregona, M. Mongiat, L. Ronconi, A. Fassina, A. Colombatti and D. Aldinucci, *Int. J. Cancer*, 2011, **128**(1), 206-215.

77. S. Dede, Supervisor: A. Karadağ, "*Synthesis, Characterization and Biological Activities of Novel Complexes Containing Dicyanidoaurate(I)*" Master Thesis, Gaziosmanpaşa Unv., Turkey, 2014.

78. Stoe & Cie (2002). X-Area (Version 1.18) and X-Red32 (Version 1.04), Stoe & Cie, Darmstadt, Germany, 2001.

79. G. M. Sheldrick, SHLEXS-97 and SHELXL-97. Program for Refinement of Crystal Structures, University of Göttingen, Germany, 1997.

80. K. Brandenburg, DIAMOND, Demonstrated Version. Crystal Impact GbR, Bonn, 2005.

81. J. M. Andrews, *J. Antimicrobial Chemotherapy*, 2001, 48, 5-16.

82. B. H. Cadirci and S. Citak, *Gazi University Journal of Science*, 2010, **23**(2), 119-123.

83. I. Wiegand, K. Hilpert and R. E. W. Hancock, *Nature Protocols*, 2008, **3**(2), 163-175.

84. L. Boyanova, G. Gergova, R. Nikolov, S. Derejian, E. Lazarova, N. Katsarov, I. Mitov and Z. Krastev, *J. Medical Microbiology*, 2005, **54**, 481-483.

85. M. Tripathi, N. K. Dubey and A. K. Shukla, World J. Microbiol. Biotechnol., 2008, **24**(1), 39-46.

86. Leora Software, *Polo-PC a user's guide to Probit or Logit analysis*, 1119 Shattuck Avenue, Berkeley, CA, 1994.

87. American Type Culture Collection, http://www.lgcstandardsatcc. org/Products/Cells_and_Microorganisms/Cell_Lines.aspx?geo_country=tr, (accessed October 2012).

88. A. Murphy, A. Vines and G. J. McBean, *Biochim. Biophys. Acta*, 2009, **2**, 551-558.

89. A. N. Yoshimoto, C. Bernardazzi, A. J. V. Carneiro, C. C. S. Elia, C. A. Martinusso, G. M. Ventura, M. T. L. Castelo-Branco, and H. S. P. de Souza, *PLoS One*, 2012, **7**(9), e45332.

90. J. Gong, F. Traganos and Z. Darzynkiewicz, *Anal. Biochem*., 1994, **218**, 314-319.

